

© 2015

Chinmay Pathak

ALL RIGHTS RESERVED

**A FLUORESCENCE SPECTROSCOPY AND FLUORESCENCE
ANISOTROPY INVESTIGATION OF THE HETEROAGGREGATION OF
ALGINATE MICROPARTICLES AND CHITOSAN NANOPARTICLES**

by

CHINMAY PATHAK

A thesis submitted to the

Graduate School – New Brunswick

Rutgers, The State University of New Jersey

In partial fulfillment of the requirements

For the degree of

Master of Science

Graduate Program in Chemical and Biochemical Engineering

Written under the direction of

Dr. Nina C. Shapley

And approved by

New Brunswick, New Jersey

May, 2015

ABSTRACT OF THE THESIS

A fluorescence spectroscopy and fluorescence anisotropy investigation of the heteroaggregation of alginate microparticles and chitosan nanoparticles

BY: CHINMAY PATHAK

Thesis Director:

Dr. Nina C. Shapley

Heteroaggregation is the aggregation in a mixed particle system where particles differ in size, chemical composition and charge. This heteroaggregation phenomenon has great importance in the natural environment as well as in industrial processes. The heteroaggregates have a wide range of applications such as particle stabilization, drug delivery and encapsulation. Previous studies of heteroaggregates have involved rigid spherical particles. In this work, we have used hydrophilic hydrogel particles which are oppositely charged and soft. These hydrogel particles, in particular, chitosan and alginate, have gained interest due to their biodegradability and nontoxicity as well as multiple delivery mechanisms. This study focuses on understanding the heteroaggregation behavior of chitosan

nanoparticles and alginate microparticles and several factors affecting their interaction.

Fluorescence spectroscopy was used to characterize and identify boundaries between several heteroaggregate morphologies, or “phases,” in the system of chitosan nanoparticles and alginate microparticles. Optical microscopy was used to observe the aggregate phases formed by fluorescently tagged chitosan nanoparticles mixed with alginate microparticles. The effect of the concentration ratio of alginate microparticles and chitosan nanoparticles was also explored.

Next, the interaction between these particles was studied for varying pH of the system as pH is an important factor where micro- and nanoparticles are used as a drug delivery system. The interaction behavior was examined regarding the changes in solution ionic strength. Furthermore, fluorescence anisotropy, which is correlated to mobility, was used to observe aggregates’ formation with varying concentration and pH. Finally, fluorescence spectroscopy was performed *in situ* in a vial containing an alginate-chitosan system.

ACKNOWLEDGEMENTS

I have received guidance and support from many people during my graduate studies, and they have my sincerest gratitude for their help. First I would like to thank my advisor, Dr. Nina Shapley, for her continuous support and wonderful guidance for my master's research. I would like to thank Dr. Maria Corradini for her valuable inputs for this project. I have learnt a lot of things from her. Special thanks to her, and Dr. Ludescher for providing access to the fluorescence spectrometer.

Next, I would like to thank Kapil Deshpande and Samyukta Budumuru who helped me start this project. I would like to thank Anik Chaturbedi and Vipul Sharma for their help with my experiments and discussions which led to fruitful ideas. I would also like to thank my fellow lab mates Shiwen Sun, Nimish Patil, Adam Cham, Christopher Dobrzanski, Yanru Yu, Nike Isijola; my department colleagues, Sarang Oka, Jennifer Winkler, Kurt Smith for their help. I am thankful to the undergraduate students that I have mentored, Brian Schendt, Yaxi Xu, Erin Dippold and, my roommates Yadvaindera Sood, Bandhan Wagheliya, Swapnil Sarode and Atish Kulkarni. Finally, I would like to thank my friends and my family for their continuous support throughout my education and our Sadhguru for his blessings without which I couldn't have reached this stage.

I dedicate this work to my late grandfather, Mr. Vasant Rao Pathak and my late aunt, Mrs. Shraddha Pathak who left our family for the unknown journey. They would have been more than happy to see me achieve my goals.

PUBLICATIONS

Parts of this work are awaiting publication and must be acknowledged.

Chapter 3 is in preparation for submission:

**Deshpande, K. V., Pathak, C., Liu, J., Budumuru, S., Corradini, M.;
and Shapley, N.C.** “Fluorescence spectroscopy characterization of
heteroaggregates of alginate microbeads and chitosan nanoparticles.”

Table of Contents

ABSTRACT OF THE THESIS	ii
ACKNOWLEDGEMENTS	iv
PUBLICATIONS.....	v
Table of Contents	vi
List of Tables	ix
List of Figures.....	x
Chapter 1 INTRODUCTION	1
1.1 Motivation.....	2
1.2 Background	4
1.2.1 Encapsulation Using Chitosan and Alginate	5
1.2.2 Fluorescence spectroscopy	11
1.2.3 Fluorescence Anisotropy	14
1.2.4 Laser Diffraction Scattering	17
Chapter 2	18
ANALYSIS OF INTERACTIONS BETWEEN CHITOSAN NANOPARTICLES AND ALGINATE MICROPARTICLES USING FLUORESCENCE SPECTROSCOPY AND ANISOTROPY	18
2.1 Introduction	19
2.2 Materials	19

2.3 Experimental Procedure	20
2.3.1 Preparation of FITC-labeled and plain Chitosan nanoparticles	20
2.3.2 Preparation of Alginate beads	21
2.3.3 Measuring Labeling Efficiency	22
2.3.4 Preparation of Samples	23
2.3.5 Preparation of Blanks	25
2.3.6 Fluorescence Spectroscopy	25
2.3.7 Microscopy	26
2.3.8 Fluorescence Anisotropy	26
2.3.9 Laser Diffraction Spectroscopy	26
2.4 pH Variation Study	27
2.4.1 Introduction	27
2.4.2 Sample preparation	29
2.5 Ionic Strength Study	30
2.6 <i>In Situ</i> measurements	31
Chapter 3 RESULTS AND DISCUSSION	32
3.1 Results for standard samples with no HCl added	33
3.1.1 Boundaries between interaction phases of chitosan and alginate	33
3.1.2 Fluorescence Spectroscopy Results	40
3.1.3 Fluorescence Anisotropy	51

3.1.4 Laser Diffraction Spectroscopy	55
3.1.5 Particle Interaction Calculations	58
3.2 Results for pH 2.3	66
3.2.1 Optical Microscope Imaging.....	66
3.2.2 Fluorescence Spectroscopy	72
3.2.3 Fluorescence Anisotropy	73
3.3 Results for pH 7	77
3.3.1 Microscope imaging.....	77
3.3.2 Fluorescence spectroscopy.....	82
3.3.3 Fluorescence Anisotropy	83
3.4 Comparison of Fluorescence Anisotropy and Intensity among the three pH Systems	84
3.5 Results for ionic strength studies	89
3.6 <i>In Situ</i> measurements.....	99
3.7 Summary	100
Chapter 4 CONCLUSIONS AND FUTURE WORK	102
4.1 Conclusions	103
4.2 Future Work.....	105
REFERENCES.....	107

List of Tables

Table 1 Levels of alginate, chitosan and water along with the pH values for each sample	24
Table 2 Values of percentage dissociation and protonation for all the three cases	87

List of Figures

Figure 1-1 A schematic representation of various heteroaggregates: A: Dissimilar particles with a large size ratio; B: Dissimilar particles of the same size. [2].....	2
Figure 1-2 Chemical structure of chitosan [20].....	6
Figure 1-3 Cross-linking of chitosan with tripolyphosphate (TPP) [20].....	7
Figure 1-4 Structure of fluorescein isothiocyanate, FITC [30]	8
Figure 1-5 Schematic illustration of the chemical synthesis of FITC-labeled chitosan [30]	9
Figure 1-6 Chemical structure of alginate [35].....	10
Figure 1-7 Egg-box structure of an alginate gel formed by chelation of Ca ²⁺ ions [38]	10
Figure 1-8 Schematic diagram of spectrofluorometer [39].....	12
Figure 1-9 Schematic diagram for measurement of fluorescence anisotropy [39]16	
Figure 3-1 Microscope image of a sample mixture of 1.45×10 ⁵ (0.003125 g) alginate particles and 1.22×10 ¹¹ (25 μL) chitosan particles.....	35
Figure 3-2 Microscope image of a sample mixture of 2.89×10 ⁵ (0.00625 g) alginate particles and 1.22×10 ¹¹ (25 μL) chitosan particles.....	36
Figure 3-3 Microscope image of a sample mixture of 5.78×10 ⁵ (0.0125 g) alginate particles and 1.22×10 ¹¹ (25 μL) chitosan particles.....	37
Figure 3-4 Microscope image of a sample mixture of 1.16×10 ⁶ (0.025 g) alginate particles and 1.22×10 ¹¹ (25 μL) chitosan particles.....	37
Figure 3-5 Microscope image of a sample mixture of 2.31×10 ⁶ (0.05 g) alginate particles and 1.22×10 ¹¹ (25 μL) chitosan particles.....	38

Figure 3-6 Microscope image of a sample mixture of 4.63×10^6 (0.1 g) alginate particles and 1.22×10^{11} (25 μL) chitosan particles.....	39
Figure 3-7 Microscope image of a sample mixture of 9.26×10^6 (0.2 g) alginate particles and 1.22×10^{11} (25 μL) chitosan particles.....	39
Figure 3-8 Microscope image of a sample mixture of 1.85×10^7 (0.4 g) alginate particles and 1.22×10^{11} (25 μL) chitosan particles.....	40
Figure 3-9 Raw spectrum for 2.31×10^6 (0.05 g) alginate particles and 1.22×10^{11} (25 μL) chitosan particles.....	41
Figure 3-10 Spectrum generated for different amounts of tagged chitosan	42
Figure 3-11 Comparison of spectra data obtained with filter and without filter for 2.31×10^6 (0.05 g) alginate particles mixed with 1.22×10^{11} (25 μL) tagged chitosan particles	43
Figure 3-12 Comparison of spectra data obtained at two different slit width for 4.63×10^6 (0.1 g) alginate particles and 1.22×10^{11} (25 μL) chitosan particles.....	44
Figure 3-13 Comparison of spectra obtained with sample containing 2.31×10^6 (0.05 g) alginate particles mixed with 1.22×10^{11} (25 μL) tagged chitosan particles and the one with 2.31×10^6 (0.05 g) alginate particles only	45
Figure 3-14 Spectra for 5.78×10^5 (0.0125 g) alginate particles mixed with 1.22×10^{11} (25 μL) tagged chitosan particles and 1.22×10^{11} (25 μL) plain chitosan particles. A corrected spectrum is obtained by subtracting non-fluorescent readings from fluorescent readings.	46
Figure 3-15 Average maximum intensity plotted against the ratio of alginate to chitosan particles with points for the interaction regime transitions from	

dispersed, coated to agglomerated (solid) and agglomerated to dispersed, uncoated (dashed) circled.	47
Figure 3-16 Plot of the slope of the average maximum intensity curve from alginate/chitosan ratio to alginate/chitosan ratio.....	50
Figure 3-17 Average anisotropy values plotted against alginate/chitosan particle ratio	52
Figure 3-18 Normalized maximum intensity and averaged anisotropy values plotted against the alginate/chitosan particle ratio	54
Figure 3-19 Particle size distribution for sample mixture of 9.26×10^6 (0.2 g) alginate particles and 1.22×10^{11} (25 μ L) chitosan particles.....	56
Figure 3-20 Particle size distribution for different levels of alginate particles and chitosan particles corresponding to three different interaction regimes.....	57
Figure 3-21 Mean particle diameter plotted against the ratio of alginate to chitosan particles with points for the interaction regime transitions from dispersed coated to agglomerated (dotted) and agglomerated to dispersed uncoated (dashed) marked with rectangles.....	58
Figure 3-22 DLVO curves for A: two interacting alginate particles and B: two interacting chitosan particles.....	62
Figure 3-23 Microscope image of a sample mixture of 1.45×10^5 (0.003125 g) alginate particles and 1.22×10^{11} (25 μ L) chitosan particles for pH 2.3	67
Figure 3-24 Microscope image of a sample mixture of 2.89×10^5 (0.00625 g) alginate particles and 1.22×10^{11} (25 μ L) chitosan particles for pH 2.3	67
Figure 3-25 Microscope image of a sample mixture of 5.78×10^5 (0.0125 g) alginate particles and 1.22×10^{11} (25 μ L) chitosan particles for pH 2.3	68

Figure 3-26 Microscope image of a sample mixture of 1.16×10^6 (0.025 g) alginate particles and 1.22×10^{11} (25 μ L) chitosan particles for pH 2.3	69
Figure 3-27 Microscope image of a sample mixture of 2.31×10^6 (0.05 g) alginate particles and 1.22×10^{11} (25 μ L) chitosan particles for pH 2.3	70
Figure 3-28 Microscope image of a sample mixture of 4.63×10^6 (0.1 g) alginate particles and 1.22×10^{11} (25 μ L) chitosan particles for pH 2.3	70
Figure 3-29 Microscope image of a sample mixture of 9.26×10^6 (0.2 g) alginate particles and 1.22×10^{11} (25 μ L) chitosan particles for pH 2.3	71
Figure 3-30 Microscope image of a sample mixture of 1.85×10^7 (0.4 g) alginate particles and 1.22×10^{11} (25 μ L) chitosan particles for pH 2.3	72
Figure 3-31 Average maximum intensity plotted against alginate/chitosan particle ratio for pH 2.3.....	73
Figure 3-32 Average anisotropy values plotted against the alginate/chitosan particle ratio	74
Figure 3-33 Average anisotropy and normalized intensity values plotted against the alginate /chitosan particle ratio.....	75
Figure 3-34 Microscope image of a sample mixture of 1.45×10^5 (0.003125 g) alginate particles and 1.22×10^{11} (25 μ L) chitosan particles for pH 7	77
Figure 3-35 Microscope image of a sample mixture of 2.89×10^5 (0.00625 g) alginate particles and 1.22×10^{11} (25 μ L) chitosan particles for pH 7	78
Figure 3-36 Microscope image of a sample mixture of 5.78×10^5 (0.0125 g) alginate particles and 1.22×10^{11} (25 μ L) chitosan particles for pH 7	78
Figure 3-37 Microscope image of a sample mixture of 1.16×10^6 (0.025 g) alginate particles and 1.22×10^{11} (25 μ L) chitosan particles for pH 7	79

Figure 3-38 Microscope image of a sample mixture of 2.31×10^6 (0.05 g) alginate particles and 1.22×10^{11} (25 μ L) chitosan particles for pH 7	80
Figure 3-39 Microscope image of a sample mixture of 4.63×10^6 (0.1 g) alginate particles and 1.22×10^{11} (25 μ L) chitosan particles for pH 7	80
Figure 3-40 Microscope image of a sample mixture of 9.26×10^6 (0.2 g) alginate particles and 1.22×10^{11} (25 μ L) chitosan particles for pH 7	81
Figure 3-41 Microscope image of a sample mixture of 1.85×10^7 (0.4 g) alginate particles and 1.22×10^{11} (25 μ L) chitosan particles for pH 7	81
Figure 3-42 Average maximum intensity plotted against alginate/chitosan particles	82
Figure 3-43 Anisotropy for pH 7 plotted against alginate/chitosan particle ratio	83
Figure 3-44 Average anisotropy and normalized intensity values plotted against the alginate /chitosan particle ratio.....	84
Figure 3-45 Anisotropy values for pH 2.3, No HCl and pH 7.0 samples plotted against the alginate/chitosan particle ratio	85
Figure 3-46 Average maximum intensity values for pH 2.3, no HCl and pH 7.0 plotted against the alginate/chitosan particle ratio	88
Figure 3-47 Normalized intensity plotted against alginate/chitosan particle ratio for different conditions	90
Figure 3-48 Microscope image of a sample mixture of 1.45×10^5 (0.003125 g) alginate particles and 1.22×10^{11} (25 μ L) chitosan particles for 0.01 M NaCl.....	92
Figure 3-49 Microscope image of a sample mixture of 2.89×10^5 (0.00625 g) alginate particles and 1.22×10^{11} (25 μ L) chitosan particles for 0.01 M NaCl.....	92

Figure 3-50 Microscope image of a sample mixture of 5.78×10^5 (0.0125 g) alginate particles and 1.22×10^{11} (25 μ L) chitosan particles for 0.01 M NaCl.....	93
Figure 3-51 Microscope image of a sample mixture of 1.16×10^6 (0.025 g) alginate particles and 1.22×10^{11} (25 μ L) chitosan particles for 0.01 M NaCl.....	94
Figure 3-52 Microscope image of a sample mixture of 2.31×10^6 (0.05 g) alginate particles and 1.22×10^{11} (25 μ L) chitosan particles for 0.01 M NaCl.....	95
Figure 3-53 Microscope image of a sample mixture of 4.63×10^6 (0.1 g) alginate particles and 1.22×10^{11} (25 μ L) chitosan particles for 0.01 M NaCl.....	95
Figure 3-54 Microscope image of a sample mixture of 9.26×10^6 (0.2 g) alginate particles and 1.22×10^{11} (25 μ L) chitosan particles for 0.01 M NaCl.....	96
Figure 3-55 Microscope image of a sample mixture of 1.85×10^7 (0.4 g) alginate particles and 1.22×10^{11} (25 μ L) chitosan particles for 0.01 M NaCl.....	96
Figure 3-56 Microscope image of a sample mixture of 1.85×10^7 (0.4 g) alginate particles and 1.22×10^{11} (25 μ L) chitosan particles for 0.1 M NaCl.....	97
Figure 3-57 Microscope image of a sample mixture of 1.85×10^7 (0.4 g) alginate particles and 1.22×10^{11} (25 μ L) chitosan particles for 0.5 M NaCl	98
Figure 3-58 Normalized intensity plotted against the alginate/chitosan particle ratio for the <i>in situ</i> measurements.....	99

Chapter 1

INTRODUCTION

1.1 Motivation

Aggregation in colloidal dispersions, suspensions and emulsions is important for several natural phenomena as well as industrial processes. Particles suspended in a medium tend to collide, and as a result of these collisions, particles aggregate or rebound off one another [1]. Aggregation can be classified into two broad categories as homo-aggregation or hetero-aggregation, depending on the similarity of particles [2]. Hetero-aggregation is aggregation of dissimilar particles, where colloidal particles may differ in size, charge and chemical composition [3]. If there is a large difference in particle size, smaller particles tend to adsorb on to the surface of larger particles. When the whole surface is covered, the surface properties of larger particles become similar to those of smaller ones [2].

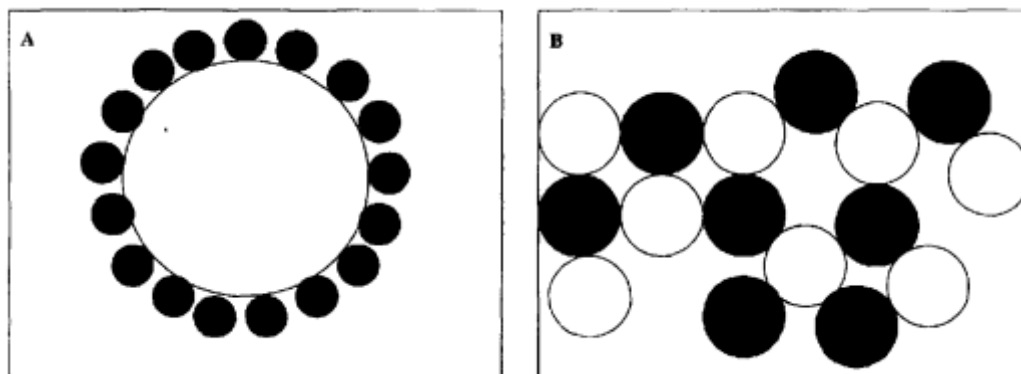


Figure 1-1 A schematic representation of various heteroaggregates: A: Dissimilar particles with a large size ratio; B: Dissimilar particles of the same size. [2]

Recently, heteroaggregates in which microparticles are coated with nanoparticles have gained renewed interest [4]. This microparticles coated with

nanoparticles assembly has several important applications. These structures can be used as flocculating agents in water purification or encapsulating harmful toxins [5]. They can also be used as particle stabilizers [6]. Another application involves their use in the pharmaceutical industry as a drug delivery system [7]. The study of heteroaggregation is more complex than that of homoaggregation, due to complexities resulting from mixing of different particulates, which makes its investigation in routine applications difficult.

Since the early 1990s, heteroaggregation studies have been carried out on systems containing oppositely charged particles [3]. Former studies of heteroaggregates have involved rigid spherical particles where at least one type is hydrophobic. In contrast, the model system used in this study consists of hydrophilic hydrogel particles which are soft, and there has not been much study of aggregation involving hydrogel microparticles and nanoparticles. The electrostatic interaction between chitosan nanoparticles and alginate microparticles is large compared to van der Waals interactions, which is the opposite of the usual case where hydrophobic particles are present. Chitosan and alginate are both biocompatible polymers and are naturally abundant with potential applications in food, environmental and pharmaceutical systems.

The aim of this thesis is to understand the heteroaggregation behavior of chitosan nanoparticles and alginate microparticles and the influence of several factors on their interaction. Transitions between distinct heteroaggregate morphologies were determined. The factors studied were the concentration of microparticles, solution pH and ionic strength of the solution. Fluorescence

spectroscopy and optical imaging were used to perform experimental measurements.

The following section in Chapter 1 provides background information regarding the study. In Chapter 2, experimental procedures have been explained in detail. Fluorescence spectroscopy has been used to identify interactions between chitosan nanoparticles and alginate microparticles. Fluorescence anisotropy has been used to identify aggregates of the chitosan-alginate system. Chapter 3 consists of results and discussion followed by Chapter 4, which discusses future work and conclusions.

1.2 Background

Previously, in an effort to create stable multicomponent aggregates, interaction between several kinds of dissimilar particles, such as amphoteric latex particles, silica, and polystyrene particles, has been studied. In one study, the effect of zeta potential, particle size ratio and electrolyte concentration on silica and latex particles was investigated [8]. Another study investigated heteroaggregation of negatively charged polystyrene particles with positively charged poly (2-vinylpyridine) PVP microgel particles [9].

Recent heteroaggregation work mainly focuses on microparticles coated with nanoparticles, which is described by the term “nanoparticle halo.” In one such work, experiments were conducted with silica microspheres mixed with hydrous zirconia nanoparticles. It was found, using neutral charge silica, that the interaction with the zirconia can be tuned based only on the concentration and

that the nanoparticle halos can be used as a stabilizing mechanism [6]. Further studies involved a system of silica microspheres and polystyrene nanoparticles. This system also exhibited stability using nanoparticle haloing. It was observed that the different interaction regimes existed as aggregation and haloing (full surface coating) [10]. Through further investigation, it was found that there exists a middle regime where aggregation occurs and above and below that regime particles are stable [11]. Simulation work also supported the presence of three possible regimes with interacting nanoparticles and microparticles [12]. The following sections provide background information on the materials and the principles of experimental techniques utilized in this study.

1.2.1 Encapsulation Using Chitosan and Alginate

Encapsulation of compounds is a process of entrapping a compound by forming a particle around that compound. Micro- and nanoencapsulating particles have variety of applications which include drug and flavor delivery, waste and toxin removal, and protection of active ingredients from the outer environment [13] [14] [15]. Alginate and chitosan are two commonly used materials in encapsulation technology.

Chitosan, Poly [(1, 4)-D-glucose-2-amine)], is a cationic polymer obtained from partial deacetylation of chitin, an abundant polysaccharide found in crustacean shells. Chitosan is positively charged due to the prevalence of amine groups that are protonated at low pH. The degree of deacetylation (DD) and molecular weight are two fundamental parameters that can affect the properties

and functionality of chitosan [16]. These properties include solubility, viscosity, reactivity and loading properties [17] [18] [19].

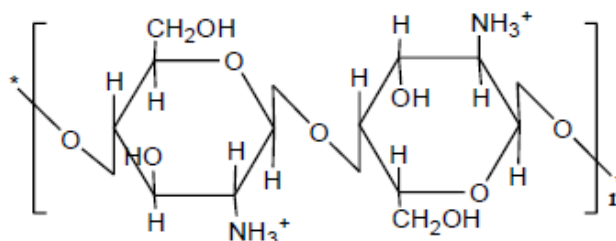


Figure 1-2 Chemical structure of chitosan [20]

With an apparent pK_a value of amino group of about 6.5, chitosan is only soluble in aqueous acidic solutions and insoluble in water and alkaline solutions [21]. When dissolved, the amino groups ($-NH_2$) of glucosamine are protonated to $-NH_3^+$. The cationic electrolyte readily interacts electrostatically with anionic groups. The cationic chitosan molecule interacts with negatively charged surfaces and anionic systems leading to modification of the physicochemical properties of these systems [22].

Chitosan has been investigated previously as a material for drug delivery and biomedical applications [23] [24]. Furthermore, due to its biocompatibility and flocculation characteristics, it is being used in food industry as an antimicrobial agent [25]. It has also been used for water purification to remove heavy metals [5].

There are various methods to produce chitosan nanoparticles which include emulsion cross linking, coacervation, spray drying, reverse micelles and

ionic gelation [7] [26]. A few reports have demonstrated water in oil microemulsion synthesis of covalently cross linked chitosan nanoparticles using glutaraldehyde as crosslinker in the size range between 30 and 150 nm [27] [28] [29].

Chitosan nanoparticles are usually produced by the ionic gelation method using sodium tripolyphosphate (TPP) as the ionic crosslinker. Resulting particles are over 100 nm diameter [7].

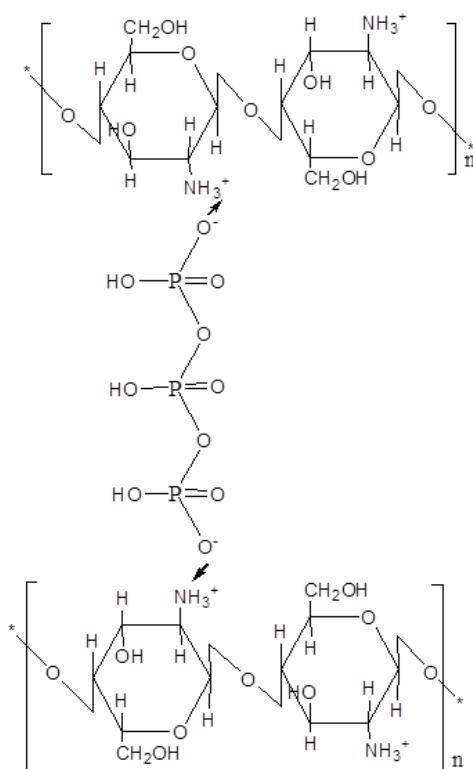


Figure 1-3 Cross-linking of chitosan with tripolyphosphate (TPP) [20]

Fluorescein isothiocyanate (FITC) is widely used to attach a fluorescent label to proteins via the amine group. The isothiocyanate group reacts with amino

terminal and primary amines in proteins. In the case of chitosan, the isothiocyanate group reacts with a D-glucosamine residue. In a previous study, FITC was used to label chitosan, and fluorescence polarization measurements of FITC-labeled chitosan were made to measure the association between chitosan and mucin [30]. In the present research, FITC has been used to label chitosan, and fluorescence spectroscopy measurements have been performed.

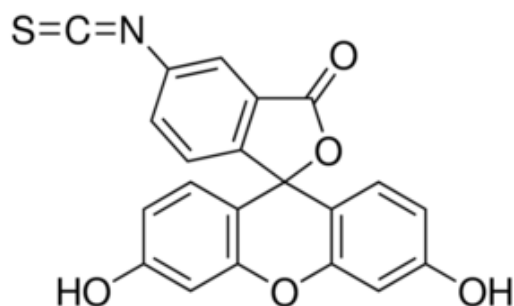


Figure 1-4 Structure of fluorescein isothiocyanate, FITC [30]

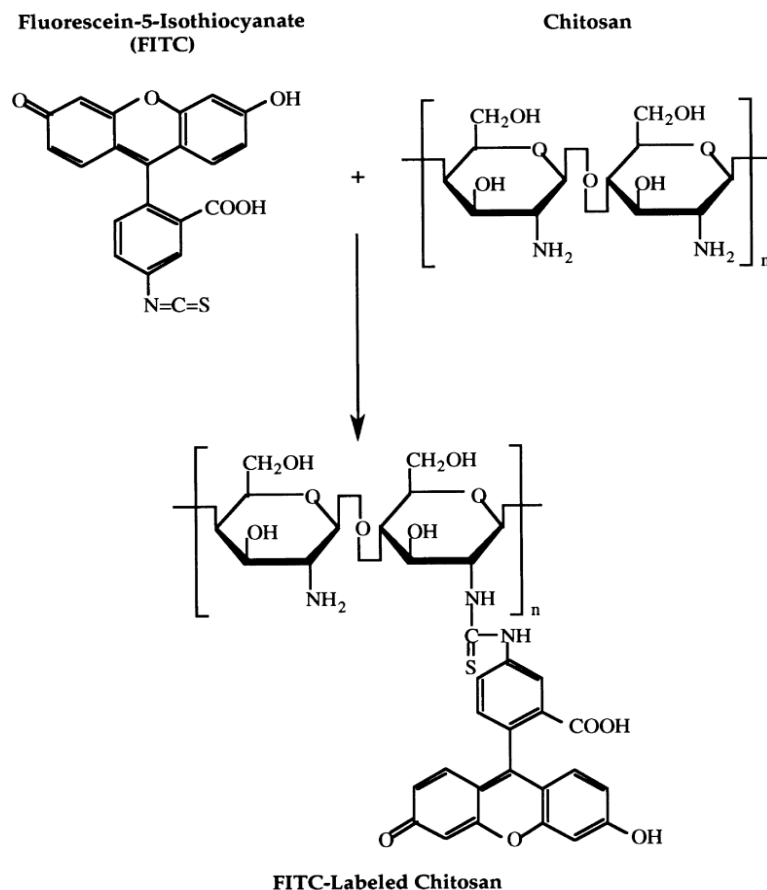


Figure 1-5 Schematic illustration of the chemical synthesis of FITC-labeled chitosan [30]

Alginate is a linear copolymer formed from mannuronic acid (M) and guluronic acid (G) subunits and is produced widely in algae. Due to its favorable properties such as biocompatibility [31], non-toxicity, biodegradability [32], it has been used in drug delivery [33], water purification [5], and food applications [34].

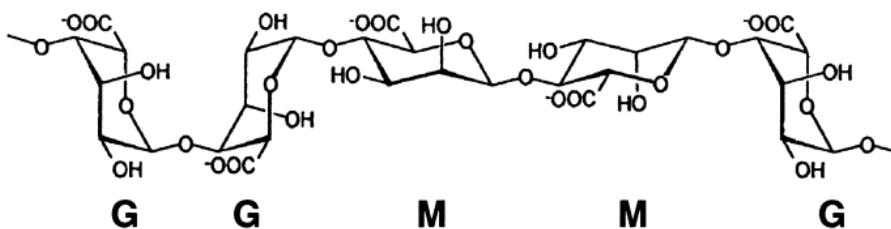


Figure 1-6 Chemical structure of alginate [35]

Alginate microparticles are produced by crosslinking with divalent ions such as Ca^{2+} . Several divalent ions like Ca^{2+} , Sr^{2+} and Ba^{2+} can be used [36]. However, Ca^{2+} provides the most stability to alginate beads [37]. The gelation and cross-linking of the polymers are mainly achieved by the exchange of sodium ions from the guluronic acids with the divalent cations and the stacking of these guluronic groups to form the characteristic egg-box structure [38] as shown in Figure 1-7.

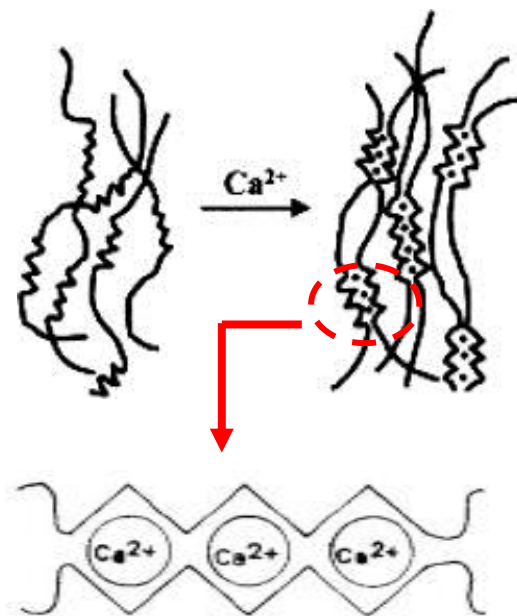


Figure 1-7 Egg-box structure of an alginate gel formed by chelation of Ca^{2+} ions [38]

1.2.2 Fluorescence spectroscopy

Fluorescence is the emission of light from a substance and occurs from electronically excited states. Fluorescence occurs in three stages, first excitation, then the excited state lifetime followed by fluorescence emission. Fluorescence spectroscopy is a technique to measure the intensity of emitted light [39].

There are two main types of fluorescence measurements: steady state and time resolved. The most commonly used type is the steady state measurement where the sample is illuminated with a continuous beam of light and an emission spectrum is recorded. Because of the nanosecond timescale of fluorescence phenomena, most measurements are steady state [39] [40]. A fluorescence emission spectrum is a plot of the fluorescence intensity versus wavelength (nanometers) or wavenumber (cm^{-1}). Fluorescence is measured by a spectrofluorometer.

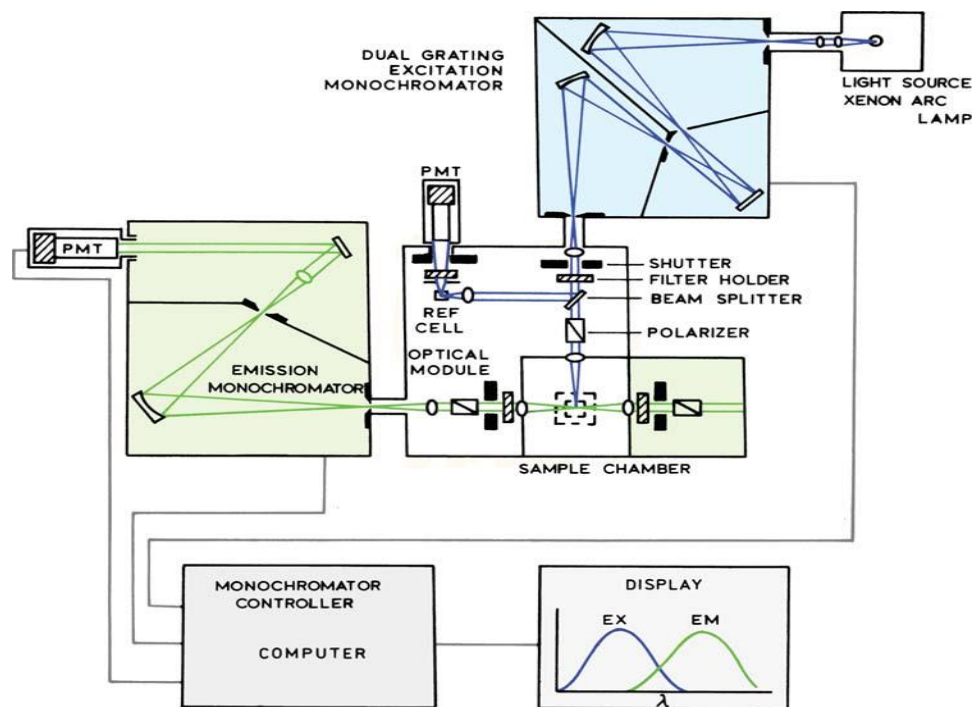


Figure 1-8 Schematic diagram of spectrofluorometer [39]

Figure 1-8 shows a schematic diagram of a general purpose spectrofluorometer. It has a xenon lamp as a source of light. Xenon lamps are useful because of their high intensity at all wavelengths from 250 nm. In this instrument, monochromators are present which allow selection of excitation and emission wavelengths. The excitation monochromator has two gratings to reduce stray light, that is, light with wavelengths different from the chosen one. For automatic scanning of wavelengths, both monochromators are motorized. The photomultiplier tubes detect fluorescence and it is quantified with appropriate electronic devices. The output is presented in graphical form and stored digitally.

Monochromators are used to disperse polychromatic or white light into the various colors or wavelengths. To achieve this dispersion, prisms or diffraction gratings are used. The monochromators in most spectrofluorometers use diffraction gratings [39].

There are various sources of light that are used in spectrofluorometers. The most versatile light source for steady state spectrofluorometer is high pressure xenon (Xe) arc lamp. These lamps provide continuous light output from 250 to 700 nm. Xenon flash lamps are used in compact fluorometers. The output is more structured than the continuous lamp. Other types include high pressure mercury (Hg) lamps, Xe-Hg arc lamp, Quartz-Tungsten Halogen (QTH) lamps and LED light sources [39].

Optical filters are used in addition to monochromators, to compensate for the inadequacy of monochromators. Often, the major source of error in all fluorescence measurements is interference due to scattered light, stray light or sample impurities. These problems can be minimized by using proper filters [39].

Spectra generated from fluorescence spectroscopy are highly dependent on the properties of fluorescing molecules or fluorophores [40]. Fluorophores are fluorescent chemical substances which emit light upon excitation by light absorption. The information available from experiments is determined by the properties of fluorophores. There are two main classes: intrinsic and extrinsic [39]. Intrinsic fluorophores are naturally occurring and include aromatic amino acids, NADH and flavins. Extrinsic fluorophores are added to give fluorescence to

samples which do not employ molecules that are inherently fluorescent [41]. Examples include dansyl, fluorescein and rhodamine [39] [41]. Fluoresceins are widely used as extrinsic fluorophores. Factors that should be considered when choosing extrinsic fluorophores are the labeling efficiency, behavior in surrounding medium and stokes shift.

Fluorescence spectroscopy has been mainly used for biological applications. Other applications include food [42] and pharmaceutical applications [43]. Fluorescence spectroscopy has been used to study interactions between DNA and metal ions [44] as well as interaction between drug and serum albumin [45]. Cell uptake of Gd (III) encapsulated chitosan nanoparticles has been studied using fluorescence spectroscopy [46]. Thus, fluorescence spectroscopy has already been used for chitosan nanoparticles. Recently, our group member developed fluorescence spectroscopy for studying particle interactions involving chitosan nanoparticles [47]. This thesis is a continuation of the previous research.

1.2.3 Fluorescence Anisotropy

Fluorescence anisotropy is an important tool for biochemical and medical applications. Anisotropy measurements provide information regarding molecular shape and size and viscosity of a fluorophore's environment. If there is a rotational freedom, the system exhibits lower anisotropy, while for rigid environments, anisotropy values are high. Anisotropy measurements give an insight into changes in molecular sizes of polymers and other macromolecules [39].

Polarized light striking a fluorescent molecule results in polarized fluorescence. The term anisotropy (r) is used to describe the extent of polarization of emitted light. Anisotropy is the ratio of the polarized light component to the total light intensity. In a homogenous solution, the ground state fluorophores are randomly oriented. When exposed to polarized light, fluorophores which have their absorption transition moments orientated along the electric field vector of the incident light are preferentially excited. Therefore the excited state population is partially oriented. Anisotropy measurements reveal the average angular displacement of the fluorophore that occurs between absorption and subsequent emission of photons. This angular displacement depends on the rate and extent of rotational diffusion during the lifetime of the excited state. The rate of rotational diffusion depends on the viscosity of the solvent and shape and size of the rotating molecule. The rotational rate of fluorophores in solution is dependent upon the viscous drag imposed by the solvent. Hence if the solvent viscosity is changed, it will result in a change in fluorescence anisotropy. For example, a small fluorophore in a low viscosity solvent will exhibit anisotropy close to zero as the rate of rotational diffusion will be faster than the rate of emission. A typical setup for measurement of anisotropy is shown in Figure 1-9.

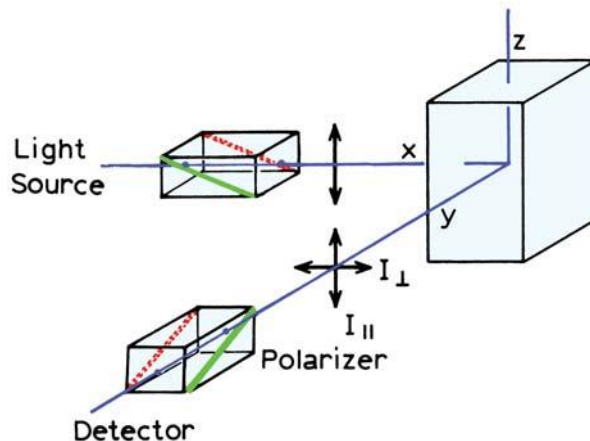


Figure 1-9 Schematic diagram for measurement of fluorescence anisotropy [39]

In fluorescence anisotropy experiments, the sample is excited with vertically polarized light. The electric field vector of the excitation light is oriented parallel to the vertical or z axis. The intensity of the emission is measured through a polarizer. When the emission polarizer is oriented parallel (\parallel) to the direction of polarized excitation, the observed intensity is called I_{\parallel} and similarly, when the polarizer is perpendicular (\perp) to the excitation the intensity is called I_{\perp} . From these intensity values, anisotropy (r) is calculated by following equation:

$$r = \frac{I_{\parallel} - I_{\perp}}{I_{\parallel} + 2I_{\perp}}$$

The anisotropy is dimensionless quantity that is independent of the total intensity of the sample.

Fluorescence anisotropy has been widely used in clinical and biomedical fields. In the past, an application of fluorescence anisotropy to study antigen-antibody interactions was developed by Dandliker. For the experiments ovalbumin was labeled with fluorescein isothiocyanate and then antibodies were raised to the fluorescein-ovalbumin adduct. Then binding of this antibody-antigen system was studied using anisotropy and intensity measurements [48]. Fluorescence polarization measurements of FITC-labeled chitosan were performed to gain better understanding of the association between chitosan and mucin in different pH and ionic conditions [30]. Recently, fluorescence anisotropy has been used for nanoparticle sizing where a particle sizing method has been developed based on analysis of rotational motion [49]. Also, it has been used for studying micellar aggregation of nonionic Brij surfactants [50]. In this study, fluorescence anisotropy has been used to study aggregation of chitosan nanoparticles and alginate microparticles.

1.2.4 Laser Diffraction Scattering

Laser diffraction scattering is a technique used for obtaining particle size distribution. Unlike other optical techniques, LDS does not require single particles to be measured successively in order to get the size distribution [51]. The method involves the analysis of the patterns of scattered light produced when particles of different sizes are exposed to a beam of light. . This technique is particularly useful for studying aggregation and dispersion phenomena. In the present study, LDS has been used to obtain the particle size distribution for mixed alginate-chitosan systems.

Chapter 2

ANALYSIS OF INTERACTIONS BETWEEN CHITOSAN NANOPARTICLES AND ALGINATE MICROPARTICLES USING FLUORESCENCE SPECTROSCOPY AND ANISOTROPY

2.1 Introduction

When oppositely charged microparticles and nanoparticles are mixed together, aggregation tends to occur and resulting aggregate morphology that occurs is dependent on particle concentration, holding other factors constant. The different regimes of particle interactions can be distinguished at boundaries according to concentration ratios. Previous studies have used optical microscopy to determine particle interaction regime boundaries. Ultra-small-angle X-ray scattering, which is not widely available, has also been used to observe aggregate morphologies [11]. However, optical microscopy has limitations as it cannot be performed *in situ* or in real time in vial or in a flow. Also, the sample, which has to be extracted and placed on a microscope slide for observation, may not accurately represent the particulate suspension. These limitations may result in a different morphology being observed compared to that present in a particulate suspension. Fluorescence spectroscopy, not having such restrictions, was used by our group member to observe interaction regime boundaries. In the present study, we have used fluorescence spectroscopy in conjunction with optical microscopy to determine interaction regime boundaries for chitosan alginate systems.

2.2 Materials

Chitosan (low molecular weight) (CAS #9072-76-4) and Sodium tri-polyphosphate (TPP) (CAS #7758-29-4, technical grade 85%) were obtained from Sigma Aldrich (St. Louis, MO). The chitosan had a deacetylation fraction of

90.85% and molecular weight range of 50-190 kDa. More specifically, the acquired batch had a viscosity of 185 cP (for a concentration of 1 w/w in 1 w/w acetic acid solution) (all data provided by supplier). Fluorescein isothiocyanate (FITC) was also acquired from Sigma Aldrich, titled- Fluorescein 5(6)-isothiocyanate BioReagent, suitable for fluorescence, mixture of two components.

Sodium Alginate (alginic acid, sodium salt, CAS #9005-38-3) was obtained from Acros Organics (Morris Plains, NJ). It had a molecular weight range of 450-550 kDa and a viscosity of 485 cP (for a 1% w/w solution) (all data provided by supplier). Furthermore, the sodium alginate contained 65-75% guluronic acid (G) subunits and 25-35% mannuronic acid (M) subunits. 1,6-dibromohexane (CAS #629-03-8, 96% purity) and Span-80 (CAS #1338-43-8) were purchased from Sigma Aldrich. Calcium chloride dihydrate FCC/USP (CAS #10035-04-8) and iso-octane (CAS #540-84-1, HPLC grade) were obtained from Fischer Scientific (Fair Lawn, NJ).

Water used for all experiments was obtained from a Milli-Q water System.

2.3 Experimental Procedure

2.3.1 Preparation of FITC-labeled and plain Chitosan nanoparticles

Chitosan was tagged with fluorescein isothiocyanate (FITC) according to the procedure outlined in Huang et al. [52]. 100 mL of chitosan solution (1% in 0.1M acetic acid) was mixed with 50 ml of solution of FITC dissolved in methanol (2.0 mg/mL) in the dark at ambient temperature followed by addition of 100 mL methanol. The solution was stirred for 3 hours to complete the tagging. After 3 h,

tagged polymer was precipitated out by adding 0.1 M NaOH solution and centrifuged at 20,000 rpm for 10 min followed by washing with methanol: water (70:30, v/v). The tagged chitosan was then redissolved in 400 mL of 0.06M Acetic acid.

FITC-labeled chitosan nanoparticles were prepared by an ionic gelation method using sodium tripolyphosphate (TPP). 0.7 mL of TPP solution (0.2 wt% in water) was added drop wise to 5 mL of tagged chitosan solution under magnetic stirring. 0.3 mL of water was then added to create a mixture of 5:1 volume ratio of chitosan and TPP. The mixture was stirred for 30 min before leaving it overnight to reach equilibrium. It was then centrifuged at 48,400 xg (20,000 rpm) for 30 min (Avanti J-E, Beckman Coulter, Brea, CA). Collected particles were suspended in water and redispersed by probe sonication (Misonix Sonicator 3000) for approximately 30 s.

For preparing plain chitosan nanoparticles, chitosan was dissolved in water with acetic acid 1.75 times the mass of chitosan to obtain a 2.0 mg/ml chitosan solution. Using this solution, plain chitosan nanoparticles were prepared by following the same ionic gelation procedure mentioned above.

2.3.2 Preparation of Alginate beads

In order to prepare alginate beads, three different solutions were prepared: Alginate solution, oil solution and calcium chloride solution. Alginate solution (2 wt%) was prepared by adding alginic acid gradually to sucrose solution in water. Oil solution consisted of 69.5% (v/v) isooctane, 29.5% (v/v) 1,6

dibromohexane, and 1 wt% span 80 surfactant. Calcium chloride solution was prepared by adding dihydrate calcium chloride (1 wt%) and sucrose (16 wt%) in water. Then equal amounts of alginate solution and oil solution were blended for 10 min at 20000 rpm (Ultra-Turrax T-25 blender, IKA works, Staufen, Germany) to form an emulsion. Cold water was used to immerse flask containing mixture to prevent overheating. The emulsified alginate was then cross-linked with calcium chloride by drop wise addition of calcium chloride solution to emulsion using fan mixer. The emulsions were then washed with acetone and separated in a separation funnel. The alginate suspension was then extracted and centrifuged at 6000 rpm at 4 °C for 10 min. Supernatant was discarded. Alginate beads thus obtained were sieved down to below 38 μm diameter and then filtered using vacuum filtration with a 25 μm pore size filter paper to get particles having diameter between 25-38 μm . These beads were stored in water.

2.3.3 Measuring Labeling Efficiency

The labeling efficiency of FITC to chitosan was determined as per the following procedure. First, the tagged chitosan solution was diluted with deionized water until a final concentration of 0.25 $\mu\text{g}/\text{mL}$ was measured. Then fluorescence intensity of that solution was measured. The calibration curve was obtained by measuring the fluorescence intensities of FITC solutions having concentration from 0.002 $\mu\text{g}/\text{mL}$ to 0.08 $\mu\text{g}/\text{mL}$. These FITC solutions were prepared by diluting methanolic solutions of FITC with deionized water. Labeling efficiency was then calculated as percent weight of FITC to weight of FITC-chitosan.

2.3.4 Preparation of Samples

Samples were prepared by mixing alginate beads with tagged chitosan particles in water. Each sample contained different amounts of alginate by weight and amount of the chitosan was kept constant (by volume). For preparing each sample, water volume was first measured out. It was kept constant at 8 ml for each sample. After that, the proper amount of alginate microparticles was added to the water. To obtain alginate beads from their storage suspension, they were centrifuged at 6000 rpm for 10 minutes in a Beckman Coulter centrifuge with the rotor. After addition of alginate to the water, all the samples were sonicated at low power (9-12 W) for 30 seconds in a probe sonicator (Misonix 3000). This was done to ensure resuspension of alginate microparticles. The next step was to add chitosan suspension to the water by measuring out the desired volume. After adding chitosan, all the samples were again sonicated at the same power. Then the samples were stirred on a stir plate using microstirbars for one hour allowing samples to cool down and reach equilibrium.

The amount of chitosan used was kept constant at 25 μL (1.22×10^{11} particles). The amounts of alginate microparticles used for each sample and corresponding pH values are shown in Table 1.

Table 1 Levels of alginate, chitosan and water along with the pH values for each sample

Sample	Chitosan Suspension Volume	Water	Alginate (g)	Number of Alginate Particles	Alginate Volume Fraction	Sample pH
1	25 μ L	7.975 mL	0	0	0	5.79
2			0.003125	1.45×10^5	3.72×10^{-4}	5.8
3			0.00625	2.89×10^5	7.44×10^{-4}	5.7
4			0.0125	5.78×10^5	1.49×10^{-3}	5.6
5			0.025	1.16×10^6	2.97×10^{-3}	5.5
6			0.05	2.31×10^6	5.95×10^{-3}	5.4
7			0.1	4.63×10^6	1.19×10^{-2}	5.17
8			0.2	9.26×10^6	2.38×10^{-2}	4.97
9			0.4	1.85×10^7	4.76×10^{-2}	4.83

The amount of alginate is doubled in each successive sample, while the chitosan volume is held constant.

2.3.5 Preparation of Blanks

For each sample, a blank was prepared. The blank is the same as the sample except it does not have the fluorophore. Blanks were prepared using plain chitosan suspension instead of FITC-tagged chitosan suspension. The preparation method of blanks is identical to the method for preparing the samples. For blank preparation, water volume was measured out first. Alginate was then added to the water followed by sonication. Then the required amount of chitosan was added to the vial. The blanks were then sonicated again and stirred for one hour before being tested with the fluorescence spectrometer. The total volume was kept constant at 8 mL for the blanks. The amount of chitosan and alginate used were the same as in Table 1.

2.3.6 Fluorescence Spectroscopy

A Horiba Jobin Vyon Fluoromax spectrophotometer was used to measure the fluorescence intensity of the samples. The instrument was calibrated before every run. For calibration, the instrument is set to excitation mode first and a reading is taken with an empty sample holder. The peak should be observed at a wavelength of 467 nm. Then emission mode is selected and signal from HPLC grade, triple distilled water is measured. The peak should occur at a wavelength of 397 nm. For measuring the intensity readings, 3 mL of each sample was taken into 4 sided clear plastic cuvettes and put inside the sample holder. Spectra were obtained by exciting the samples with incident light having wavelength of 490

nm. Emission spectra were obtained for range of 500-650 nm. Slit lengths of 5 nm and 2 nm were chosen for the experiments and a 495 nm filter was used.

Similarly, fluorescence readings were taken for blanks for each sample. These blank or non- fluorescent readings were then subtracted from sample or fluorescent chitosan readings to obtain accurate intensity reading given exclusively by the fluorophore. For each sample, three replicates were done.

2.3.7 Microscopy

Optical microscopy was performed for each sample using a Zeiss Axio Lab A1 microscope. Approximately 50 μ L of sample was spread out on a concavity slide. The image was taken using Axiovision software under 50 x magnifications.

2.3.8 Fluorescence Anisotropy

Fluorescence anisotropy was measured using a Cary Fluoromax instrument. For measurement, 3 mL of sample was taken into a cuvette and placed inside the sample holder. The sample was excited at 490 nm and the emission wavelength was set at 518 nm. A filter of 495 nm wavelength was used for the experiment. A sample with zero alginate and 25 μ L chitosan was used as a reference. For each sample, three trials were accomplished.

2.3.9 Laser Diffraction Spectroscopy

The particle size distribution was obtained by using a Beckman Coulter LS 13 320 laser diffraction particle size analyzer. The universal liquid module (ULM) was used for size measurements. The ULM measures the entire sample

introduced to the instrument by re-circulating the sample. Samples were prepared by measuring out the amount of water followed by addition of alginate. Chitosan was added after that and samples were tested immediately without sonication. The ratios of alginate to chitosan particles were kept same as mentioned in Table 1. Additional samples with similar ratios were tested to get better understanding of the size distribution. For measurements, the sample was gradually pipetted into the module until an obscuration level of eight percent was reached. Data was obtained on the basis of volume percent. The module was auto rinsed and aligned between each measurement. Samples were run for combined obscuration and polarization intensity differential scattering (PIDS) analysis. Since the laser diffraction spectroscopy measurements require dilution of the sample with large amounts of deionized water in a flow loop, they were only attempted for the standard samples with compositions listed in Table 1, without any intentional pH or ionic strength modifications.

2.4 pH Variation Study

2.4.1 Introduction

In the biomedical and biomaterials field, stimulus responsive hydrogels have found novel applications in drug delivery [53], tissue engineering [54] and biosensors [55]. The stimuli include changes in a physical property of the system such as temperature [56] [57] as well as changes in chemical properties such as pH and ionic strength of the system [58]. In particular, pH sensitive hydrogels are used in drug delivery for controlled oral administration because of the large

changes that occur in pH along the digestive track [53]. Alginate and chitosan particles have been used for drug delivery with pH tunable release. They release their payloads when pH is lowered [7] [36]. Hence it is necessary to study interaction between chitosan and alginate as pH is lowered. Interaction regime boundaries may change with pH, as zeta potential changes when pH is changed. Thus the concentration ratio of chitosan to alginate required to maintain particle stability as pH is lowered can be established by determining interaction regime boundaries. Fluorescence spectroscopy has been used to study particle interactions at different pH values. By undertaking a pH study, the applicability of fluorescence spectroscopy in different environments can be tested.

In the standard sample mixtures listed in Table 1, the resulting pH values range from 4.8 to 5.8. In the pH variation study, two comparison pH values of 2.3 and 7.0 were selected in order to vary systematically the colloidal interactions between the alginate and chitosan particles. At both pH values of 2.3 and 7.0, one of the polymers is beyond its pKa value and therefore only slightly charged and near precipitation, while the other is highly charged. A pH value of 2.3 represents a strongly acidic environment which is close to but below the pKa value of alginate (~3.5) and significantly below the pKa value of chitosan (~6.5). Therefore, we expect the alginate microparticles to be only weakly charged and the chitosan nanoparticles to be highly charged. In contrast, at pH 7.0, the system is above the pKa value of the chitosan and significantly above the alginate pKa value, so accordingly we expect highly charged alginate microparticles and weakly charged chitosan nanoparticles. At each comparison

pH, electrostatic attraction between dissimilar particles is reduced and electrostatic repulsion between similar particles of one type is enhanced, which results in a contrasting balance of colloidal forces compared to the standard samples, where both electrostatic attraction between dissimilar particles and electrostatic repulsion between similar particles are substantial.

2.4.2 Sample preparation

For the pH modified samples, 0.2M hydrochloric acid (HCl) was used. Amounts of alginate and chitosan used were the same as those mentioned in Table 1. Samples were prepared in a similar fashion mentioned in section 2.3.4. First, 6 mL of water was taken into a vial. Then an appropriate amount of alginate obtained from centrifuging an alginate suspension was added to the water. The sample was sonicated and then 25 μ L of chitosan was added to the sample. The sample was sonicated again and 0.2M HCl was added gradually until the desired pH was reached. To monitor pH value, a pH meter was used. Finally, the sample volume was made up to 8 mL by adding the required amount of DI water. For each set of modified samples, the pH was held constant at a value of either 2.3 or 7.0. For pH 7.0, 0.2M sodium hydroxide (NaOH) was used. Samples were stirred on a stir plate with microstirbars for one hour before running the fluorescence spectroscopy experiment. Blanks were prepared in exactly same way using plain chitosan nanoparticles instead of tagged ones. Blanks had same pH values as that of respective samples. Each sample was then tested with the Horiba Fluoromax spectrometer using 490 nm excitation wavelength and 495 nm filter. Emission spectra were obtained over range of 500-650 nm. A slit length of 2 nm

was used for all the experiments. Respective blank or non-fluorescent readings were subtracted from corresponding sample or fluorescent readings to get an accurate reading obtained exclusively from the fluorophore FITC. A Zeiss Axio lab A.1 microscope with 50x magnification was used to photograph samples. For each sample, three trials were performed.

2.5 Ionic Strength Study

For the ionic strength study, samples were prepared using sodium chloride (NaCl) solution. Three different salt concentrations of 0.01M, 0.1M and 0.5M were studied. The goal was to investigate the shifts in particle interaction regime boundaries due to the presence of varied concentrations of ions, which may shield electrostatic interactions between particles. NaCl solutions were prepared by mixing the appropriate amount of NaCl into DI water. For sample preparation, the appropriate volume of NaCl solution was measured out first. Alginate was centrifuged from its suspension solution and was then added to the NaCl solution. The sample was sonicated for 30 seconds before adding 25 μ L chitosan suspension to it. After adding chitosan, the sample was sonicated again at the same power. All the samples were then stirred for one hour before testing with the Horiba Fluoromax spectrofluorometer. Respective blanks were prepared by adding plain chitosan nanoparticles in place of tagged chitosan nanoparticles. Samples were excited at a wavelength of 490 nm and emission spectra were recorded from 500 nm to 650 nm. Each experiment was done using a 495 nm filter and a 2 nm slit length. For each sample, the blank reading was subtracted to

get an accurate reading. The amount of chitosan was kept constant at 25 μL and alginate amount varied as per Table 1.

2.6 *In Situ* measurements

Samples were prepared in glass vials for the *in situ* measurements. The amount of alginate and chitosan was kept the same as mentioned in Table 1. For sample preparation, first water volume was measured out which was kept constant at 8 mL. The appropriate amount of alginate was then added to the water. Samples were sonicated at low power for 30 s. Then chitosan was added to the samples and again samples were sonicated to re-disperse the particles. Measurements were performed using a fiber optics probe and the Cary Eclipse fluorometer after stirring the samples for one hour. Blank samples were prepared in a similar way using plain chitosan instead of the fluorescent chitosan. Readings were also taken for the blank samples.

Chapter 3
RESULTS AND DISCUSSION

In this chapter, results for the experiments are discussed. Section 3.1 presents the results for standard samples with no HCl added. First, the microscope images and fluorescence spectroscopy results have been discussed followed by fluorescence anisotropy and laser diffraction spectroscopy results. Each section is followed by detailed discussion of the results obtained. In sections 3.2 and 3.3, results for pH 2.3 and pH 7.0 respectively, are presented. Optical microscope results have been compared with fluorescence spectroscopy results and fluorescence anisotropy results. Finally, results and discussions for ionic strength study and *in situ* measurements are presented in sections 3.5 and 3.6 respectively. At the end, section 3.7 gives the summary of all the experiments.

3.1 Results for standard samples with no HCl added

Several optical measurement techniques were applied to standard samples, which had the compositions listed in Table 1 without any HCl added for pH modification. The complementary measurements include optical microscope imaging, fluorescence spectroscopy, fluorescence anisotropy and laser diffraction spectroscopy. The results acquired from the standard samples are presented in this section along with relevant controls and data analysis.

3.1.1 Boundaries between interaction phases of chitosan and alginate

Optical microscope imaging was used to observe different phases of interaction between chitosan nanoparticles and alginate microparticles. Microscope images were used to determine location of boundaries between the different interaction regimes. There are three different regimes as observed from

the images. The first one is dispersed coated regime where alginate microparticles are coated with chitosan nanoparticles. Amount of alginate is very less so that chitosan completely covers the surface of alginate particles and these particles start repelling each other to form discrete particle suspension. The second regime is agglomerated, where several alginate particles are loosely connected by many chitosan particles to form a cluster. The third regime is dispersed uncoated regime. In this regime, number of alginate particles is large compared to chitosan particles and hence there is not enough chitosan to fully cover surface of alginate particles. Alginate particles are partially coated with chitosan and there is not sufficient chitosan to form a loose connection between alginate particles leading to a cluster.

For imaging, the first alginate level tested was 1.45×10^5 (0.003125 g) particles. As shown in Figure 3-1, at a level of 1.22×10^{11} (25 μ L) chitosan particles, the alginate particles are clearly dispersed. As the amount of alginate is too low, chitosan sufficiently covers the surface of alginate particles to avoid any aggregation.

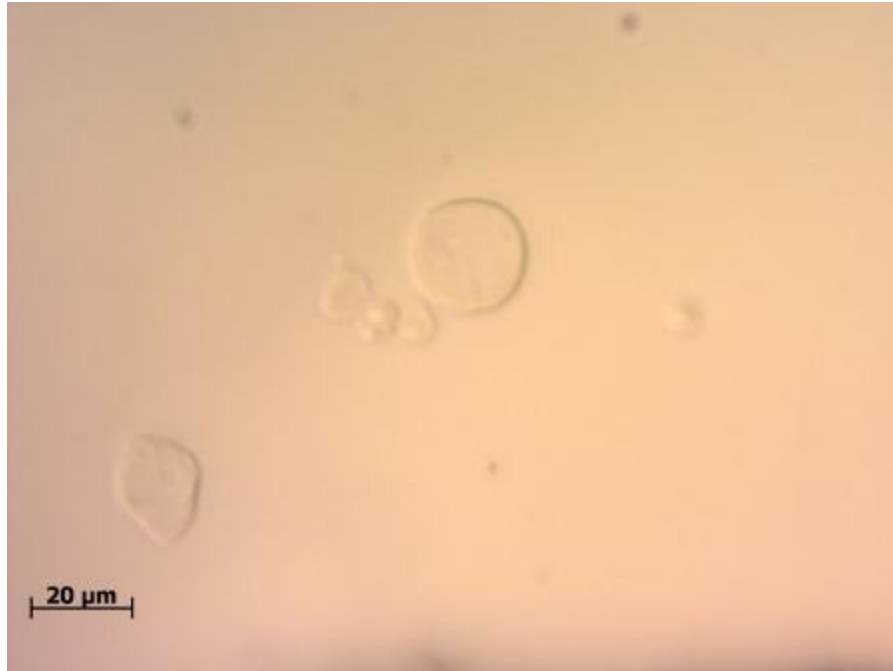


Figure 3-1 Microscope image of a sample mixture of 1.45×10^5 (0.003125 g) alginate particles and 1.22×10^{11} (25 μ L) chitosan particles

At a alginate level of 2.89×10^5 (0.00625 g) particles, first sign of borderline aggregation can be seen Figure 3-2. This level marks the boundary between dispersed, coated and agglomerated regime.

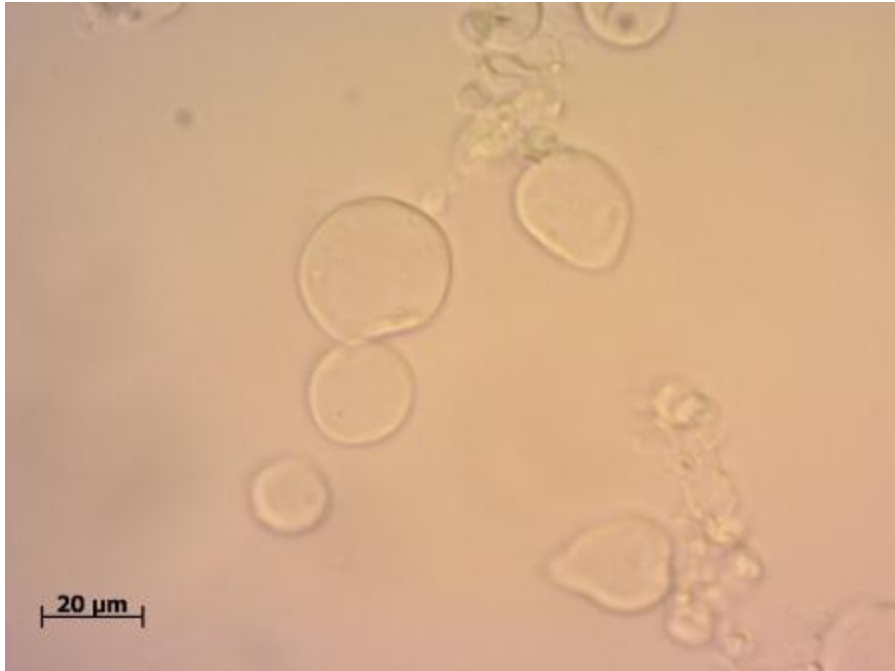


Figure 3-2 Microscope image of a sample mixture of 2.89×10^5 (0.00625 g) alginate particles and 1.22×10^{11} (25 μ L) chitosan particles

At alginate levels of 5.78×10^5 (0.0125 g) particles (Figure 3-3) and 1.16×10^6 (0.025 g) particles (Figure 3-4), we can see definite agglomeration.



Figure 3-3 Microscope image of a sample mixture of 5.78×10^5 (0.0125 g) alginate particles and 1.22×10^{11} (25 μ L) chitosan particles



Figure 3-4 Microscope image of a sample mixture of 1.16×10^6 (0.025 g) alginate particles and 1.22×10^{11} (25 μ L) chitosan particles



Figure 3-5 Microscope image of a sample mixture of 2.31×10^6 (0.05 g) alginate particles and 1.22×10^{11} (25 μ L) chitosan particles

At 2.31×10^6 (0.05 g) particles, we see that the particles are starting to disperse again (Figure 3-5). This level marks the regime boundary between agglomerated and dispersed, uncoated.

The dispersed, uncoated regime continues through the alginate levels of 4.63×10^6 (0.1 g) and 9.26×10^6 (0.2 g) to 1.85×10^7 (0.4 g) alginate particles as seen in Figure 3-6, Figure 3-7 and Figure 3-8 respectively.

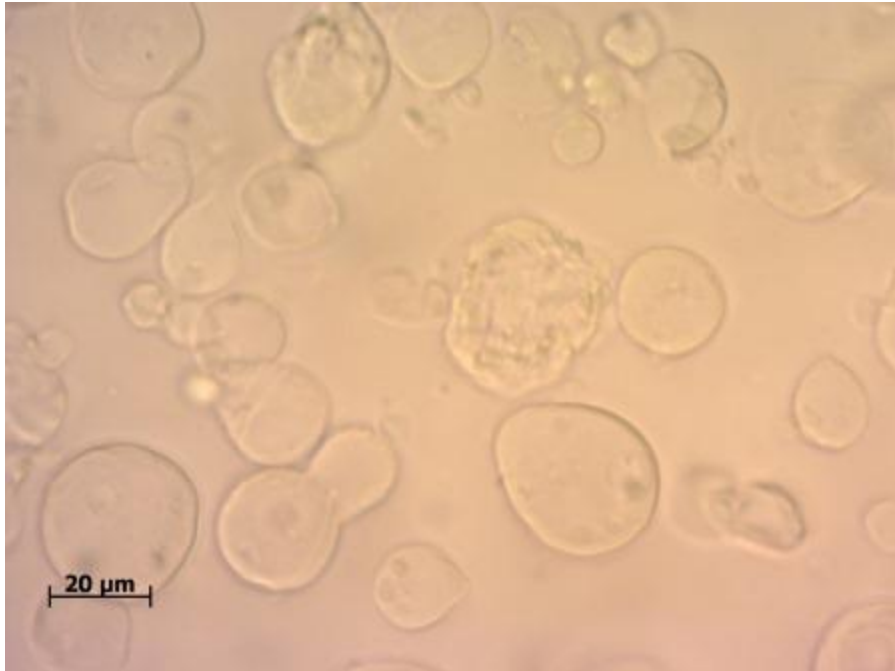


Figure 3-6 Microscope image of a sample mixture of 4.63×10^6 (0.1 g) alginate particles and 1.22×10^{11} (25 μL) chitosan particles



Figure 3-7 Microscope image of a sample mixture of 9.26×10^6 (0.2 g) alginate particles and 1.22×10^{11} (25 μL) chitosan particles



Figure 3-8 Microscope image of a sample mixture of 1.85×10^7 (0.4 g) alginate particles and 1.22×10^{11} (25 μ L) chitosan particles

As seen in Figure 3-8, the number of alginate particles is very large compared to that of chitosan nanoparticles and there are not enough chitosan particles to cover alginate surface or to form loosely connected alginate particle clusters. Alginate particles push each other to remain dispersed in the suspension.

3.1.2 Fluorescence Spectroscopy Results

The samples were tested with Horiba Jobin Vyon fluorescence spectrometer. Emission spectra were collected from 500 nm to 650 nm. Figure 3-9 shows an example of a generated spectrum.

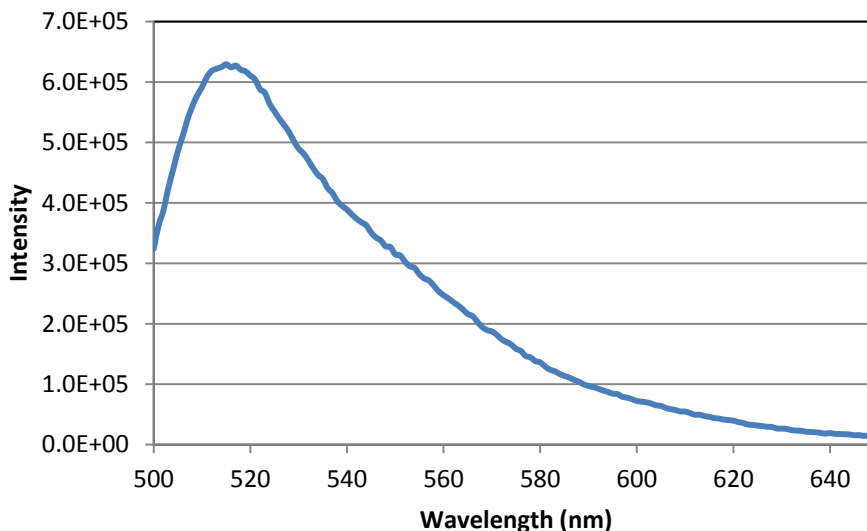


Figure 3-9 Raw spectrum for 2.31×10^6 (0.05 g) alginate particles and 1.22×10^{11} (25 μ L) chitosan particles

Fluorescence intensity is directly proportional to the concentration, typically at low concentrations. As the concentration is increased, different factors affect intensity such as the inner filter effect or collision quenching. At intermediate concentrations, the sample material at the surface of the cuvette near the light source absorbs most of the light so there is not much light available for the rest of the sample. Thus readings will not be linear. When the concentration is too high, light cannot pass through the sample to cause excitation which results in reduced intensity. Also, self-quenching may occur at high concentrations causing reduction in intensity.

Hence to determine if the concentration of tagged chitosan used was in linear range or not, fluorescence spectroscopy of samples containing different amounts of tagged chitosan only was performed.

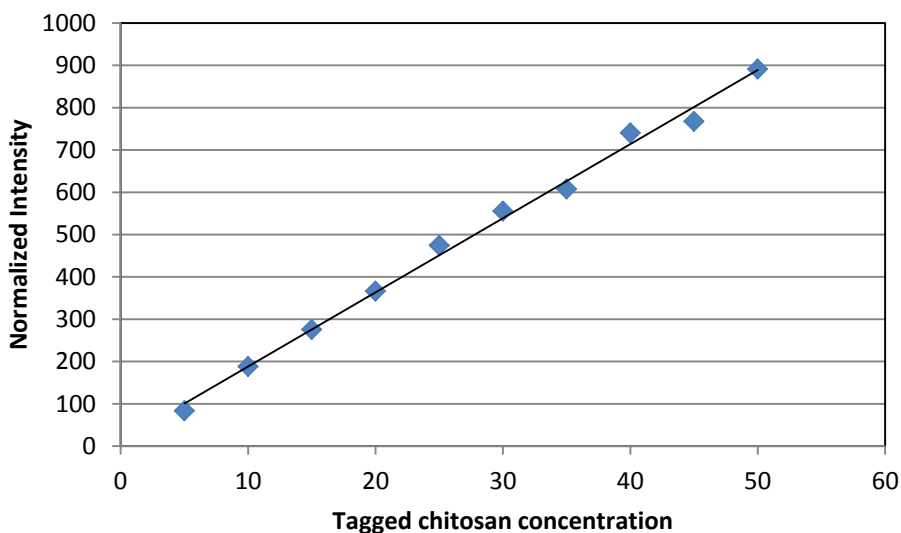


Figure 3-10 Spectrum generated for different amounts of tagged chitosan (0-50 μL) with no alginate

From Figure 3-10, it is clear that the concentration of chitosan used (25 μL) was in the linear range.

To minimize the interference caused by scattered light, optical filter of wavelength 495 nm was used. This filter selectively transmits light below 495 nm which is then absorbed by the fluorophore. Figure 3-11 shows an example of fluorescence spectrum obtained with filter and without filter.

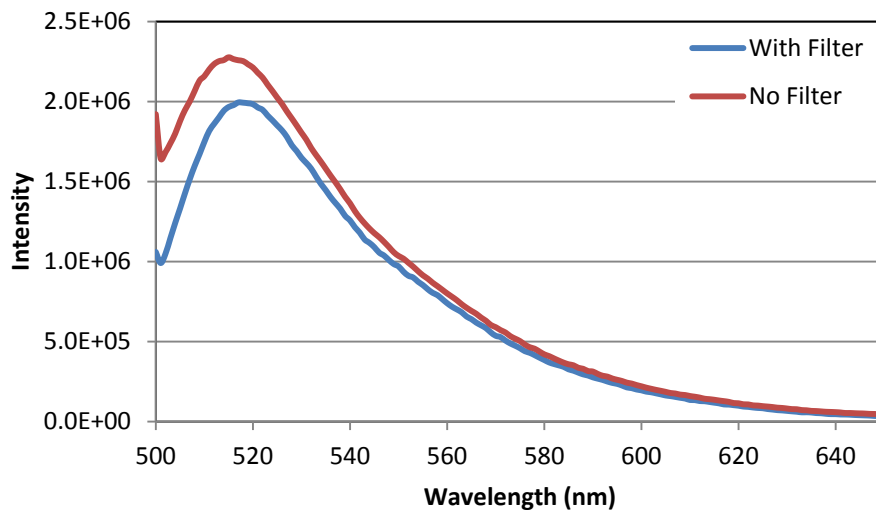


Figure 3-11 Comparison of spectra data obtained with filter and without filter for 2.31×10^6 (0.05 g) alginate particles mixed with 1.22×10^{11} (25 μL) tagged chitosan particles

It can be clearly seen from the figure that the scattering is substantially reduced with the help of the filter.

In order to get intensity values within the limit of the Fluoromax instrument, measurements were performed at different slit lengths. Figure 3-12 shows example of spectra obtained at different slit lengths.

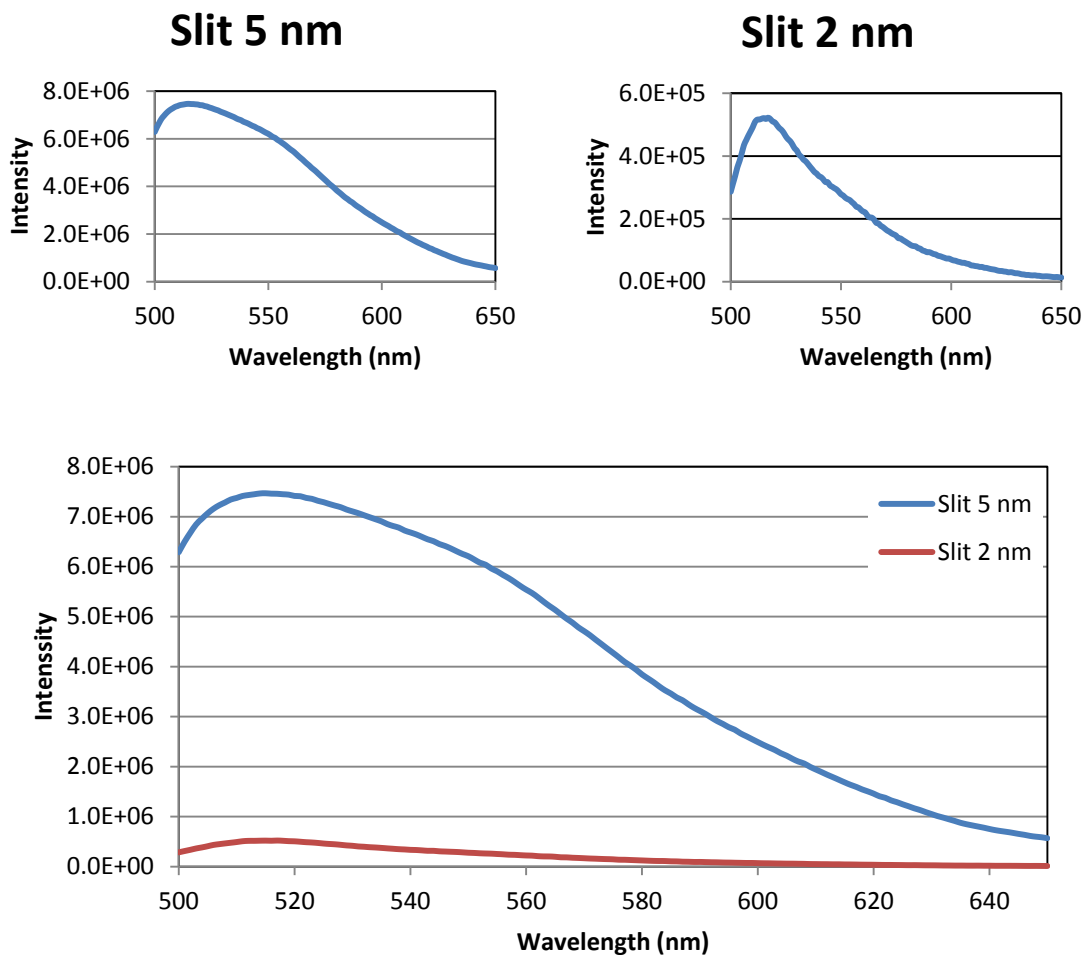


Figure 3-12 Comparison of spectra data obtained at two different slit width for 4.63×10^6 (0.1 g) alginate particles and 1.22×10^{11} (25 μ L) chitosan particles

The intensity of the light passing through the monochromators is proportional to square of slit width. The slit acts like volume control for the light intensity. Large slit width means higher signal levels and smaller slit width yields better resolution. In the Figure 3-12, it can be clearly seen that at slit width of 5 nm we obtained very high intensity as compared to that obtained with slit width of 2 nm. For Fluoromax spectrometer, the upper detection limit for the intensity is around ten million. The operating range should be within three percent of this

limit. As we can see, for slit width of 5 nm, the observed intensity is near the upper limit. Hence it was not used as it may damage the spectrometer. Hence for all the experiments, slit width of 2 nm was used.

In order to confirm that the fluorescence signal was obtained from only the FITC fluorophore and not the alginate particles, samples containing alginate particles only were tested with spectrofluorometer. As shown in Figure 3-13, fluorescence intensity observed for alginate particles is negligible in comparison with the samples containing alginate particles with fluorescent chitosan particles. Hence it was confirmed that the alginate particles are not contributing to the observed fluorescence intensities.

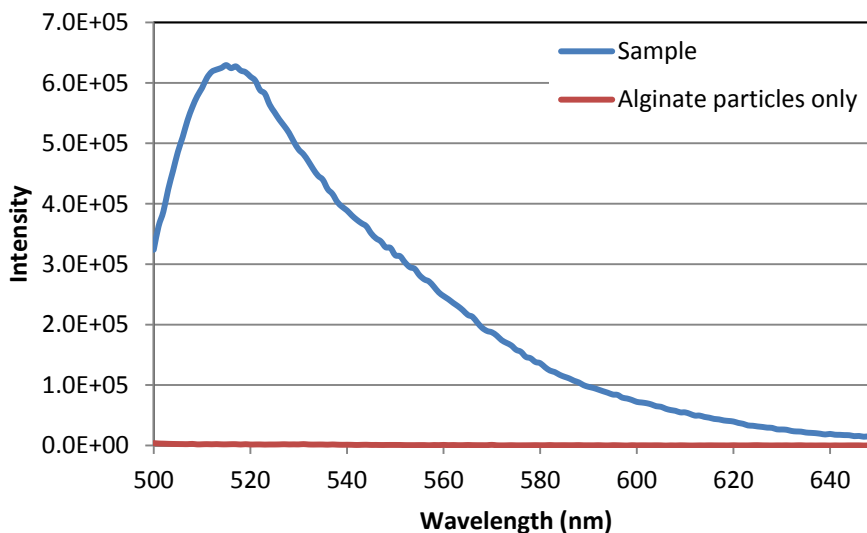


Figure 3-13 Comparison of spectra obtained with sample containing 2.31×10^6 (0.05 g) alginate particles mixed with 1.22×10^{11} (25 μ L) tagged chitosan particles and the one with 2.31×10^6 (0.05 g) alginate particles only

Fluorescence spectroscopy measurements were performed for both the samples and blanks. In order to obtain accurate readings, blank or non-fluorescent readings were subtracted from sample or fluorescent readings. An example of fluorescent and non-fluorescent readings is shown in Figure 3-14.

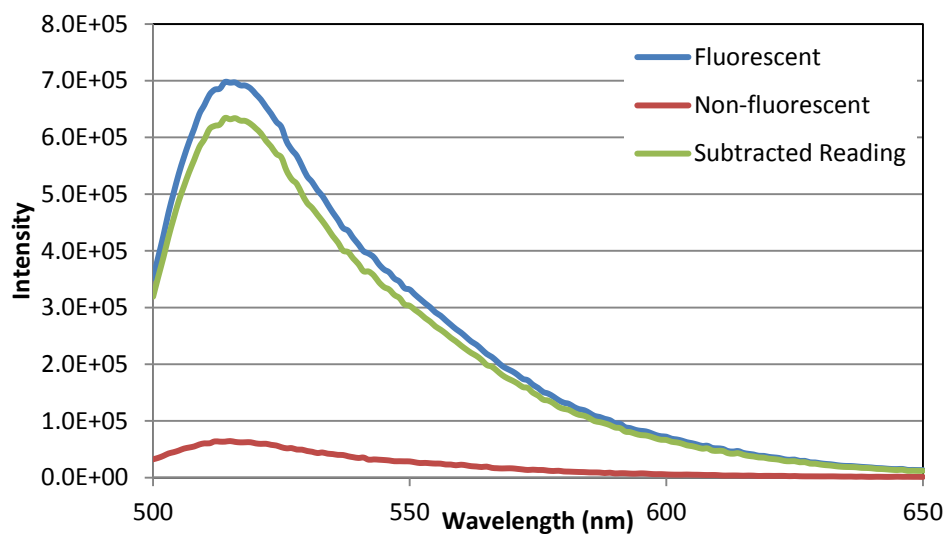


Figure 3-14 Spectra for 5.78×10^5 (0.0125 g) alginate particles mixed with 1.22×10^{11} (25 μL) tagged chitosan particles and 1.22×10^{11} (25 μL) plain chitosan particles. A corrected spectrum is obtained by subtracting non-fluorescent readings from fluorescent readings.

For each spectrum, maximum intensity values were calculated and these intensities were averaged over 3 trials for each level of chitosan and alginate. The results for constant chitosan and varying alginate are shown in Figure 3-15.

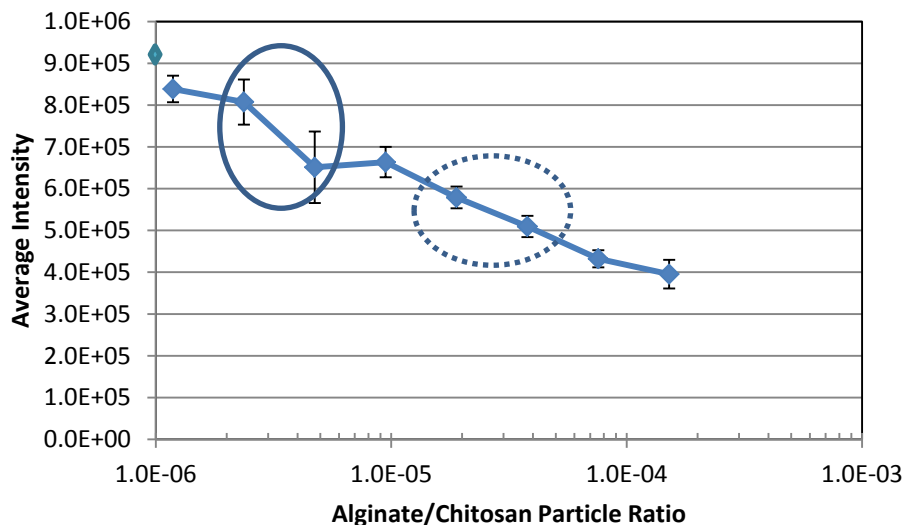


Figure 3-15 Average maximum intensity plotted against the ratio of alginate to chitosan particles with points for the interaction regime transitions from dispersed, coated to agglomerated (solid) and agglomerated to dispersed, uncoated (dashed) circled.

The intensity values of alginate in all the three regimes: dispersed coated, agglomerated and dispersed uncoated are lower than that of the control with zero alginate. The transition of interaction regime from dispersed coated to agglomerated is indicated by a significant drop in signal intensity at a low number of alginate particles. However, the transition from agglomerated to dispersed uncoated is not as definitive from the plot. This transition is denoted by a smooth curve which decreases first and then nearly plateaus. The signal intensity continues to drop as the number of alginate particles increases and reaches a plateau near the end. The fact that the intensity keeps on decreasing from the control value indicates that fluorescence quenching or scattering from alginate particles is responsible for the decrease in the intensity.

As observed from the microscope images, the transition from the dispersed coated regime to the agglomerated regime is quite abrupt. Fluorescence spectroscopy results corroborate this observation. In the control sample, only tagged chitosan is present. As soon as we start adding alginate microparticles, fluorescence intensity goes down. One of the possible reasons for this reduction is a local pH effect. pH is known to change in close proximity to a charged surface and the extent of the change is proportional to the surface potential [59]. Negative surface potentials induce a lower surface pH compared to the bulk pH, while positive surface potentials induce higher surface pH.

In the case of standard samples, alginate is highly negatively charged, which results in lower values of local pH compared to the bulk pH, which in turn results in reduced intensity as fluorescence intensity decreases with pH. Initially, in the dispersed coated phase, there are very few alginate particles and hence tagged chitosan nanoparticles will be sufficient to coat the alginate particles. Only a small fraction of the chitosan nanoparticles that contain the fluorophores will be located in close proximity to the reduced pH alginate surfaces. Most of the tagged chitosan nanoparticles are in free suspension and therefore produce a full intensity signal. As more and more alginate particles are added to the system, an increasing fraction of the tagged chitosan nanoparticles are found in close proximity to the reduced pH alginate surfaces, leading to reduction in the fluorescence signal intensity. In the agglomerated regime, there is significant coating of alginate particles but also the formation of large clusters of tagged chitosan nanoparticles that are not all in direct contact with alginate, as well as

another portion of tagged chitosan nanoparticles in free suspension. At the highest levels of alginate particles identified with the dispersed uncoated regime, chitosan is not at all sufficient to coat the alginate particles or to form clusters. Accordingly, virtually all of the tagged chitosan nanoparticles are directly adsorbed on to the reduced pH alginate surfaces. In addition, because the negatively charged alginate surfaces are only partially coated, the mostly unshielded alginate particles may induce lower local pH values than those of the dispersed coated phase and agglomerated phase. As the pH value at the surface is lower, the fluorescence intensity is less. Hence, the intensity values from the dispersed uncoated phase are lower than that of the dispersed coated phase or agglomerated phase.

Another possible reason for the reduction in fluorescence intensity with increasing alginate concentration is self-quenching. Self-quenching takes place when two or more fluorophores are in close proximity of each other [59]. In the agglomerated phase, there are free chitosan particles inside the aggregates which are close to each other. This results in self-quenching causing reduction in the intensity. In the dispersed uncoated phase, the chitosan particles are attached to alginate particles which are very close to each other causing more self-quenching. However, in the dispersed coated phase, there are many free chitosan particles repelling each other because of the positive charge. Accordingly, self-quenching is present to a lower extent than in the other regimes.

To gain understanding, and quantify the interaction regime boundaries, the slope of the normalized average intensity was calculated. For calculations, the

change in the normalized average intensity was divided by change in the concentration of alginate particles. A plot of these values was created to determine the slope where the interaction regime boundary is indicated.

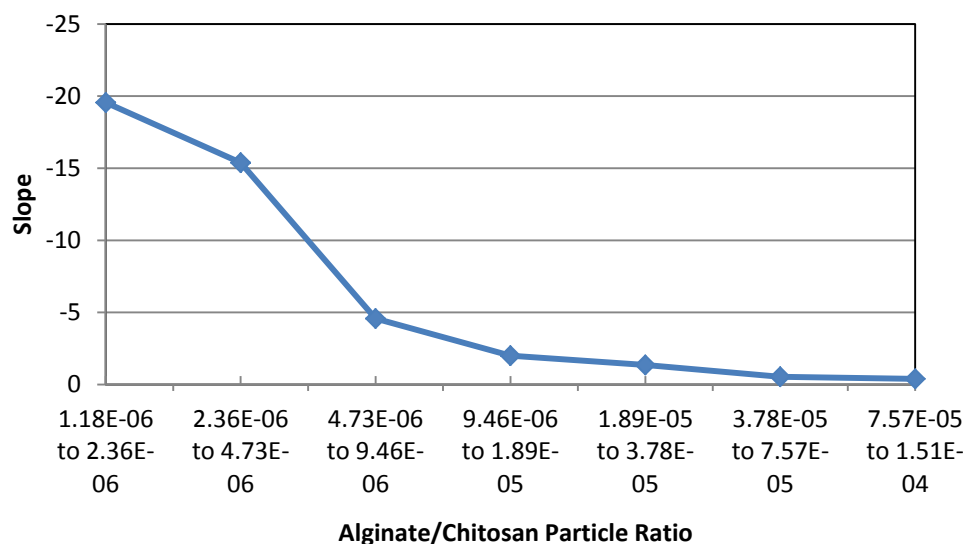


Figure 3-16 Plot of the slope of the average maximum intensity curve from alginate/chitosan ratio to alginate/chitosan ratio

From this plot, it can be observed that the interaction regime change from dispersed coated to agglomerated regime is indicated by sharp drop in the slope value from -15 to -5. However, there is no clear indication of regime change from the agglomerated to the dispersed uncoated regime, as the slope values are almost identical. Thus the interaction boundary regime threshold for the switch from dispersed coated to agglomerated phase is marked by the slope value of -15. The meaning of this value is that significant local pH changes or self-quenching

are evident in the changing intensity values. The fluorescent chitosan particles come into closer contact with alginate particles and with each other as the transition to the agglomerated regime occurs.

3.1.3 Fluorescence Anisotropy

In order to further understand the mechanisms causing intensity reduction, samples were subjected to fluorescence anisotropy measurements. Fluorescence anisotropy uses polarized light to excite the sample and the fraction of incident light polarized by the sample is detected as the emission. Anisotropy is given as a ratio of the polarized light component to the total light intensity.

The anisotropy value, denoted by r , was obtained for each sample. A plot of anisotropy values, averaged over 3 trials, is shown in the figure below. As observed from the graph of anisotropy vs. ratio of alginate particles and chitosan particles, anisotropy stays nearly constant for small amounts of alginate particles. It increases rapidly when the number of alginate particles is more than 2.31×10^6 which corresponds to the boundary of regime transition from the agglomerated to the dispersed uncoated regime. In general, there is an upward trend in anisotropy as alginate concentration is increased.

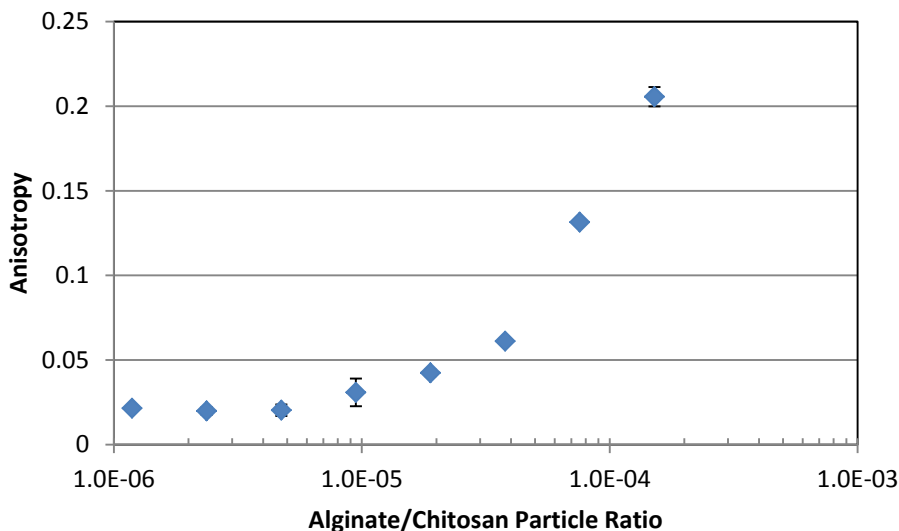


Figure 3-17 Average anisotropy values plotted against alginate/chitosan particle ratio

The trend in the anisotropy can be explained in terms of rotational diffusion. Most fluorophores in a solution rotate extensively during 50-100 picoseconds. Hence molecules can rotate many times during 1-10 nanosecond excited state lifetime and the polarized emission is randomly oriented. Due to this reason, many fluorophores in non-viscous solutions display anisotropy values near zero [39]. To put it another way, if the molecule is free to rotate during the lifetime of a fluorophore, that is, between absorption and emission, then the anisotropy values are near zero. In most cases, the rotational correlation times are comparable to the fluorescence lifetimes. As a result, measurements of fluorescence anisotropy are sensitive to any factor that changes the rotational correlational times.

In the present case, anisotropy values are near zero for the lower amounts of alginate particles and increase when the amount of alginate is higher. This phenomenon is due to the size difference between the fluorescent chitosan and alginate particles. For instance, when fluorescent chitosan is adsorbed on the alginate, the rotation is slow due to the micron sized alginate. This adsorption effectively alters the rotational correlational time and observed values of anisotropy are high. In the dispersed coated phase, the number of fluorescent chitosan particles per alginate particle is quite high as compared to that of the alginate. Hence alginate particles are coated with chitosan and still there are many free fluorescent chitosan particles in the solution. These particles, not being bound to the alginate, are free to rotate and result in near zero anisotropy values. For the agglomerated regime, most of the chitosan particles are inside the agglomerates or on the surface of the alginate. The remaining fluorescent particles in the solution are free to rotate and observed anisotropy values are similar to those obtained for dispersed coated phase. In case of the dispersed uncoated phase, all the chitosan particles are adsorbed onto the alginate surface leading to slower rotation which then leads to the high anisotropy values.

To understand how fluorescence anisotropy results compare with fluorescence spectroscopy measurements, the normalized intensity and anisotropy are plotted on the same graph. Figure 3-18 shows variation in normalized intensity and anisotropy with ratio of alginate to chitosan particles.

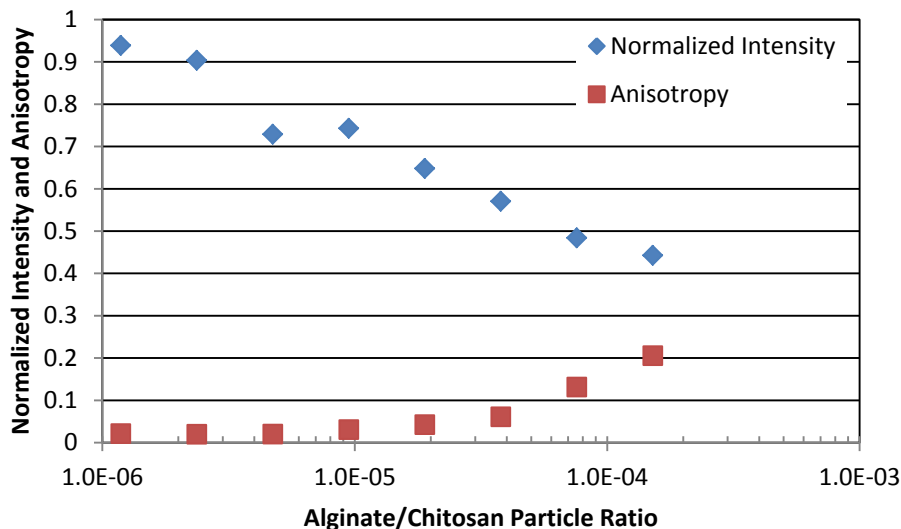


Figure 3-18 Normalized maximum intensity and averaged anisotropy values plotted against the alginate/chitosan particle ratio

From the figure, it is clear that the trend in anisotropy is exactly opposite to that of the intensity. The transition from the dispersed coated to the agglomerated regime is not clear from the anisotropy results. However, the rapid change in anisotropy for higher amounts of alginate clearly indicates a regime change. This regime change corresponds to the transition from the agglomerated to dispersed uncoated phase. Putting the two measurement methods together, we can detect both interaction regime transitions that were observed by optical microscopy.

3.1.4 Laser Diffraction Spectroscopy

Laser diffraction particle size analysis was done to improve understanding of the heteroaggregate size distribution across the regimes and to support fluorescence spectroscopy and fluorescence anisotropy results. Ideally, one should expect similar sizes for dispersed coated and dispersed uncoated regimes. Due to the presence of aggregates, particles in the agglomerated regime should be larger than the alginate particles. Also, the size range of the particles in the dispersed coated and dispersed uncoated regime is expected to be similar to that of the alginate particles. Laser diffraction spectroscopy was performed with the samples having similar ratios of alginate and chitosan particles. The particle size distribution was obtained as the change in the volume percent with respect to the particle diameter. Figure 3-19 shows an example of the particle size distribution results.

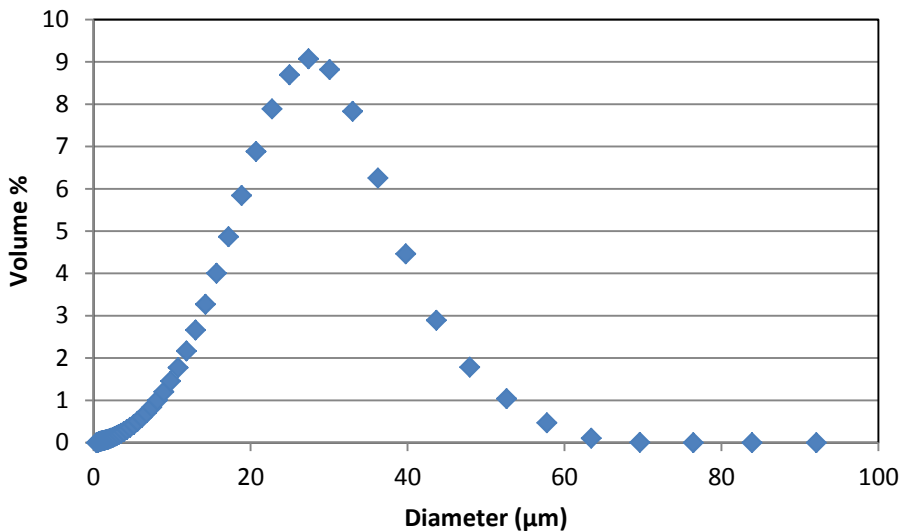


Figure 3-19 Particle size distribution for sample mixture of 9.26×10^6 (0.2 g) alginate particles and 1.22×10^{11} (25 μL) chitosan particles

With the help of particle size distribution results, the shift in the regimes can be readily observed. For the lower amount of the alginate particles as compared to the chitosan particles, a shift can be observed from the dispersed coated to the agglomerated regime. The three different regimes can be clearly seen in the Figure 3-20.

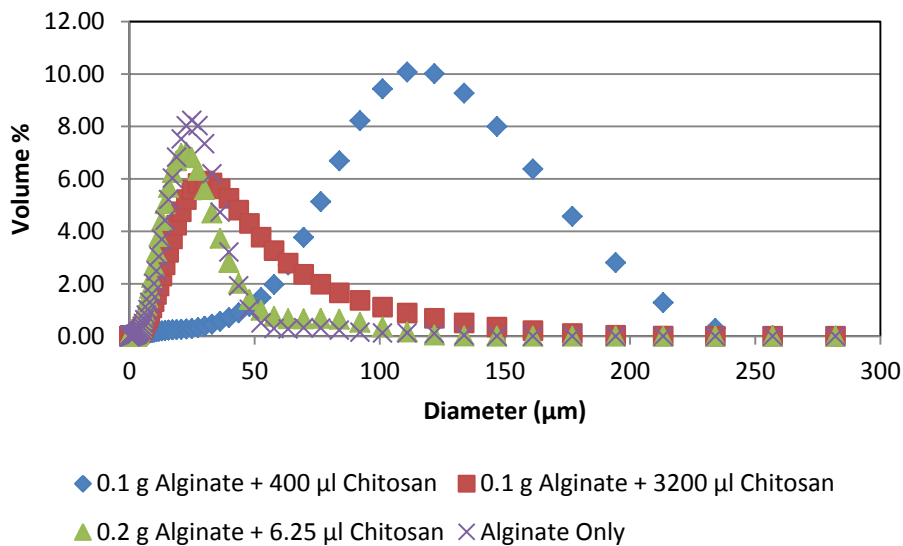


Figure 3-20 Particle size distribution for different levels of alginate particles and chitosan particles corresponding to three different interaction regimes

As observed from the Figure 3-20, the particles in the agglomerated regime are larger than those in the dispersed coated and the dispersed uncoated regimes. Also, the particles are similar in size for the dispersed coated and dispersed uncoated regimes. To get boundaries at which the interaction regime changes, the particle diameter was plotted against the ratio of the alginate and chitosan particles.

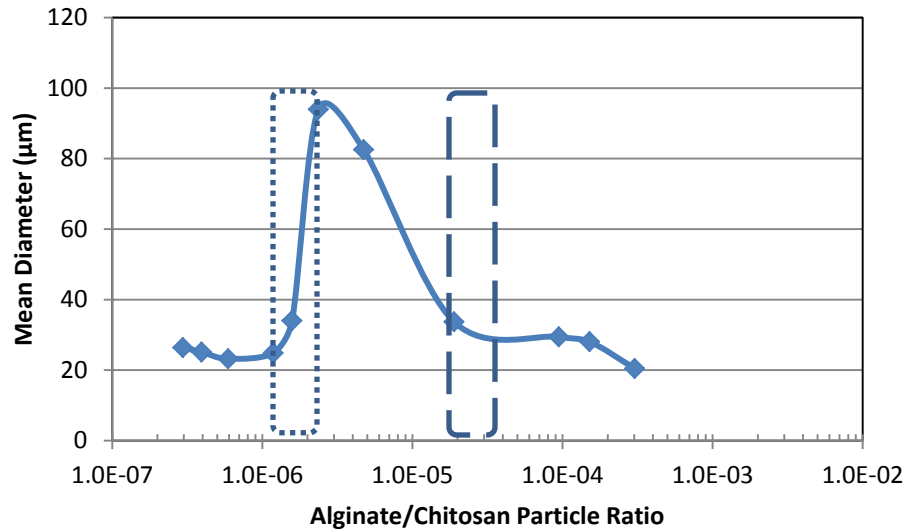


Figure 3-21 Mean particle diameter plotted against the ratio of alginate to chitosan particles with points for the interaction regime transitions from dispersed coated to agglomerated (dotted) and agglomerated to dispersed uncoated (dashed) marked with rectangles

From Figure 3-21, it is clear that the interaction regime change from the agglomerated to dispersed uncoated regime is marked by the particle ratio of 1.89×10^{-5} . The change from the dispersed coated to agglomerated regime is marked by particle ratio of 2.37×10^{-6} . This result corroborates the interaction regime boundaries indicated by optical imaging. Thus laser diffraction spectroscopy is able to provide a clear picture of all the three regime transitions.

3.1.5 Particle Interaction Calculations

In order to understand why the regime boundaries were located at the designated particle ratios, several calculations using established particle interaction theory in its simplest form were done. First, the number of chitosan

particles required to neutralize the surface charge of an alginate particle was calculated. The surface charge densities of the chitosan and alginate particles were calculated using the equation,

$$q_s = \varepsilon_3 \varepsilon_0 \zeta \left(\frac{1}{a} + \kappa \right)$$

where ε_3 is the dielectric constant of the medium, ε_0 is the vacuum permittivity, $8.85 \times 10^{-12} \text{ Fm}^{-1}$, ζ is the zeta potential, a is the radius of the particle, and κ is the inverse Debye length [60]. At room temperature, Debye parameter is given by the expression $\kappa = \sqrt{I}/0.304 \text{ nm}^{-1}$ where I refers to the ionic strength of the solution [60]. Debye length is an inverse of Debye parameter κ . For the standard samples with no HCl added, the ionic strength of the solution was approximated as 10^{-5} M , which corresponds to pH value of 5 for the chitosan suspensions. The expression for κ yields a Debye length of 96 nm.

For calculating the surface charge density of alginate, zeta potential is -46 mV [61] and average particle radius is 17 μm . For chitosan particles, zeta potential is 40 mV and average radius is 125 nm. The medium is water for both the alginate and chitosan and hence the same Debye length and dielectric constants are used. The dielectric constant of 80.1 is used for the calculations. The surface charge density was then multiplied by the surface area of the particles to get total charge of the particles. Since only one side of the chitosan particles adsorbs onto the surface of the alginate, the alginate particle is assumed to interact with only half of the surface charge of the chitosan particle. The other side of the chitosan particles is neutralized by the solution counterions. Hence

half of the total chitosan surface charge is divided by total surface charge of the alginate particles. This quotient yields an alginate to chitosan ratio of 4.14×10^{-5} . This surface neutralization ratio is very close to the experimentally determined ratios of 1.89×10^{-5} and 3.79×10^{-5} which marked the transition from dispersed uncoated to agglomerated regime. Thus the particle ratio calculations suggest that the mechanism for the transition from agglomerated to dispersed uncoated regime is charge neutralization. If the electrostatic interactions are eliminated by surface charge neutralization, then only van Der Waals forces remain, driving the particles together towards aggregation, considering the effect of other factors to be negligible.

For understanding the interactions between the particles, the total interaction potential energy was approximated by DLVO calculations. The total energy is the summation of the electrostatic repulsion energy and van Der Waals attraction energy. The electrostatic repulsion energy was calculated using the equation outlined in Israelachvili [62] for 1:1 electrolytes,

$$W_{Spheres} = 4.61 \times 10^{-11} R \gamma^2 e^{-\kappa D} \text{ J}$$

where $\gamma = \tanh \frac{e\psi}{4kT}$

Zeta potential (ζ) is used in place of surface potential (ψ) for simplicity since surface potential cannot be measured directly and cannot be accurately calculated. R is the radius of the particle, D is the distance between the particles and κ is Debye parameter.

The van der Waals attraction energy is calculated using the simple attraction of two spheres model [62],

$$W = -\frac{AR}{12D}$$

where, A is Hamaker constant having typical value of 10^{-19} J, R is the radius of particle and D is separation between the particles. This equation is valid for interacting alginate microparticles but less accurate for chitosan nanoparticles interacting with each other.

Next, in order to calculate the maximum number of particles that can fit into the control volume while still experiencing attractive interactions, the minimum stable separation distance between the particles was determined. The total interaction energy was calculated by adding electrostatic repulsion energy and van der Waals energy. The total energy was plotted as a function of distance between particles. The minimum separation distance was determined where the interaction energy changes from causing repulsion to causing attraction, that is from positive values to negative values.

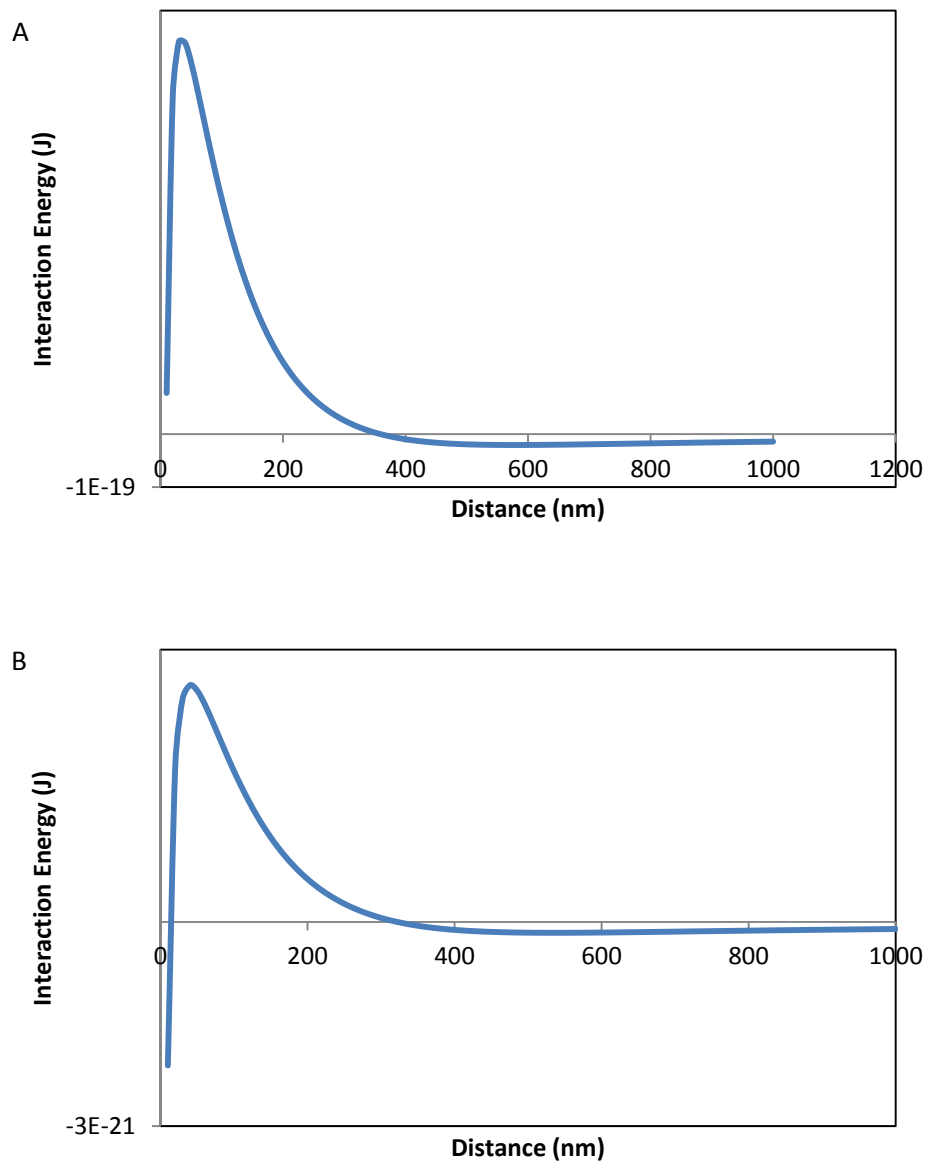


Figure 3-22 DLVO curves for A: two interacting alginate particles and B: two interacting chitosan particles

The minimum stable separation distance represents the minimum distance of attraction, while particles repel if they are placed in close proximity. For two interacting alginate particles, the minimum stable separation distance is

350 nm. For two chitosan particles, the minimum stable separation distance is 320 nm.

In order to calculate the ratio of alginate to chitosan particles in agglomerates, the maximum number of particles that can fit in a control volume of a 2 mm by 2 mm box was determined. For the calculations, a simple cubic arrangement of particles was assumed. Then, the maximum number of alginate particles that can fit in the control volume was determined using the minimum separation distance between the alginate particles. Then, the number of chitosan particles that can adsorb onto the alginate surface was determined by assuming that each chitosan particle occupies an area of πr^2 of the alginate surface area, where r is the radius of the chitosan particle. A packing factor of 0.9 (hexagonal close packing of monodispersed particles on a plane) was considered for this calculation. This number was multiplied by the total number of alginate particles to get the number of chitosan particles adsorbed on to the alginate particles. Afterwards, empty space in the control volume was calculated assuming a monolayer of adsorbed chitosan on the alginate. Finally, it was assumed that the chitosan fills up the empty space in a cubic lattice and the number of free chitosan particles was determined using the chitosan minimum stable separation distance from DLVO calculations. The ratio of alginate particles to chitosan particles in the control volume is the number of alginate particles divided by the summation of free and adsorbed chitosan particles. The calculated ratio was 3.75×10^{-6} . This ratio lies in between the experimentally determined particle ratios

of 2.37×10^{-6} and 4.73×10^{-6} that marked the transition from dispersed coated to agglomerated regime.

The estimated values of the ratio of alginate and chitosan particles suggest that there is accumulation of a large amount of unadsorbed chitosan inside the agglomerates. The ratio of unadsorbed to adsorbed chitosan particles in the control volume is 3:1. This can explain the reduced fluorescence intensity as more and more fluorescent chitosan particles are inside the agglomerate leading to fluorescence quenching.

The assumption of a chitosan monolayer on each alginate particle is very simple and does not take into account the complex nature of the interactions between the chitosan and alginate particles. For this reason, the calculated ratio is slightly higher than the experimental values. Also, the alginate and chitosan are not hard spheres but very porous hydrogels. The chitosan particles might get adsorbed completely in the alginate particle, exposing more surface area leading to higher zeta potential values which would then increase the minimum stable separation distance. A greater separation distance between alginate particles would lead to fewer number of alginate particles that can fit in the control volume which would result into lower, more accurate ratios, closer to the experimental values.

These simple approximate calculations for standard samples provide possible mechanisms for the shifting of interaction regime boundaries. For the dispersed uncoated regime, alginate particles stay dispersed as electrostatic repulsion is higher than van der Waals attraction. For the agglomerated regime,

the surface charge of alginate is neutralized resulting in lower electrostatic repulsion which is then overcome by van der Waals attraction leading to aggregates. In the dispersed coated regime, chitosan particles cannot get closer to the alginate or chitosan particles than the minimum separation distance. Hence they are unable to pack into the agglomerate, leading to the formation of dispersed coated phase.

3.2 Results for pH 2.3

This section contains results obtained from samples with a pH value of 2.3 by using the same experimental techniques described earlier. Microscope images of the samples and fluorescence spectroscopy and anisotropy measurements are presented. The goal of the pH variation study is to determine the shifts that occur in the particle interaction regime boundaries when the balance of colloidal interaction forces is altered.

3.2.1 Optical Microscope Imaging

Microscope images of the samples with the pH value of 2.3 were taken for the same levels of alginate and chitosan used in standard sample (no HCl) case (Table 1). The images show no clear interaction regime change over the concentration range studied. For the alginate levels of 1.45×10^5 (0.003125 g) and 2.89×10^5 (0.00625 g), the particles are well dispersed as seen in the Figure 3-23 and Figure 3-24 respectively.

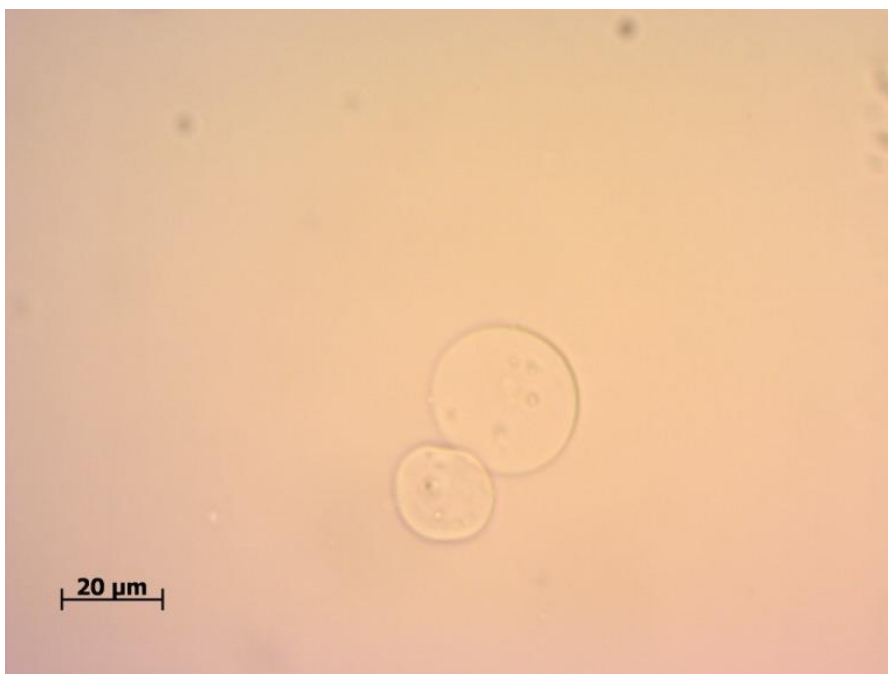


Figure 3-23 Microscope image of a sample mixture of 1.45×10^5 (0.003125 g) alginate particles and 1.22×10^{11} (25 μL) chitosan particles for pH 2.3



Figure 3-24 Microscope image of a sample mixture of 2.89×10^5 (0.00625 g) alginate particles and 1.22×10^{11} (25 μL) chitosan particles for pH 2.3

For the alginate levels of 5.78×10^5 (0.0125 g) and 1.16×10^6 (0.025 g), again particles are in dispersed state which can be clearly observed from the Figure 3-25 and Figure 3-26 respectively. This observation is in contrast with that of the no HCl case. In the standard sample (no HCl) case, these two points were in the agglomerated regime.

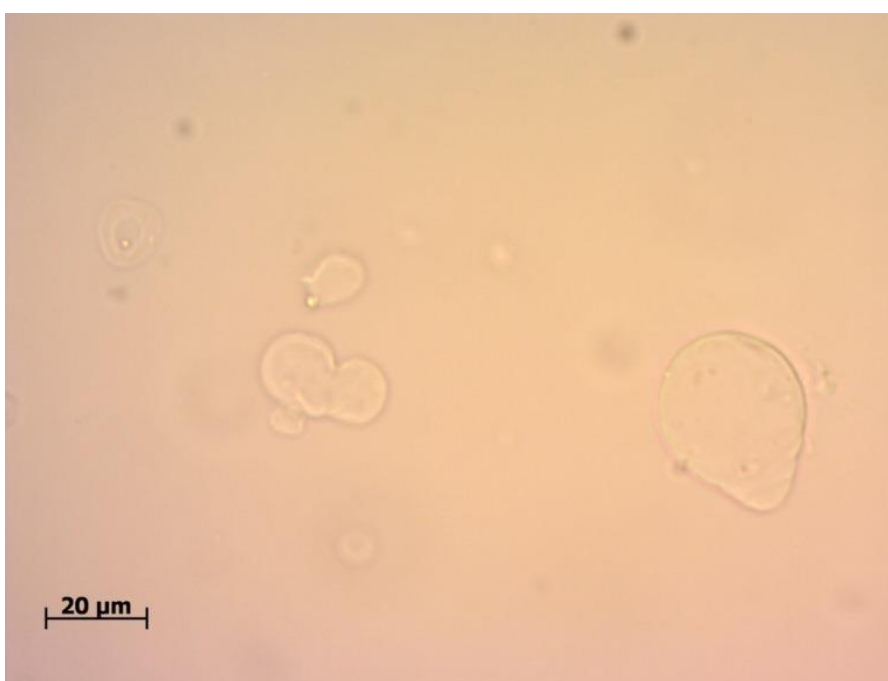


Figure 3-25 Microscope image of a sample mixture of 5.78×10^5 (0.0125 g) alginate particles and 1.22×10^{11} (25 μ L) chitosan particles for pH 2.3



Figure 3-26 Microscope image of a sample mixture of 1.16×10^6 (0.025 g) alginate particles and 1.22×10^{11} (25 μL) chitosan particles for pH 2.3

The Figure 3-27 shows the microscope image for the alginate level of 2.31×10^6 (0.05 g). This point corresponded to the regime change from the agglomerated phase to the dispersed uncoated phase for the standard samples with no HCl added. Here the particles are clearly dispersed and there is no sign of any aggregation. The image for alginate level of 4.63×10^6 (0.1 g) also indicate that the particles are in dispersed uncoated phase (Figure 3-28).

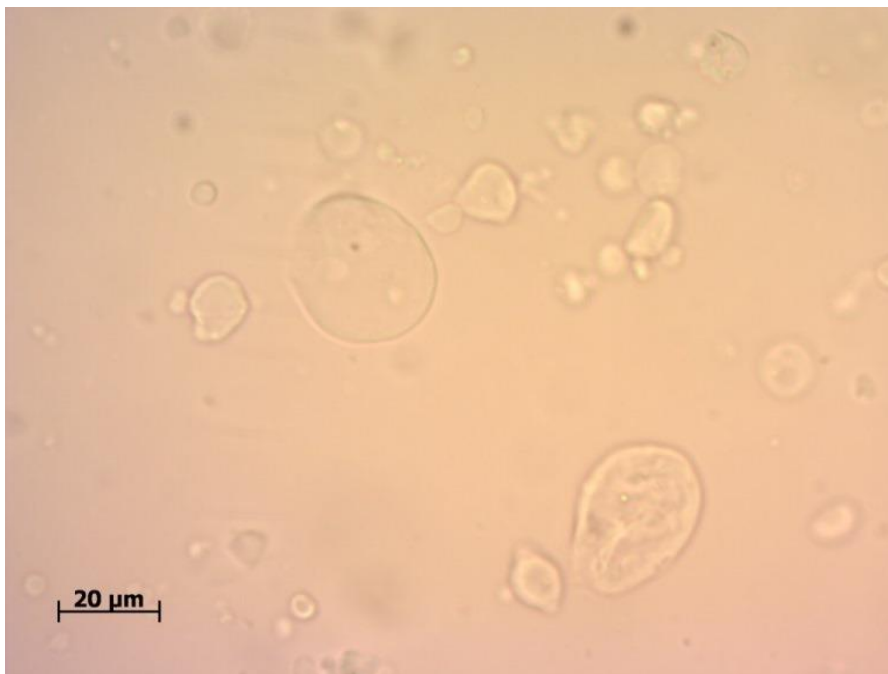


Figure 3-27 Microscope image of a sample mixture of 2.31×10^6 (0.05 g) alginate particles and 1.22×10^{11} (25 μL) chitosan particles for pH 2.3

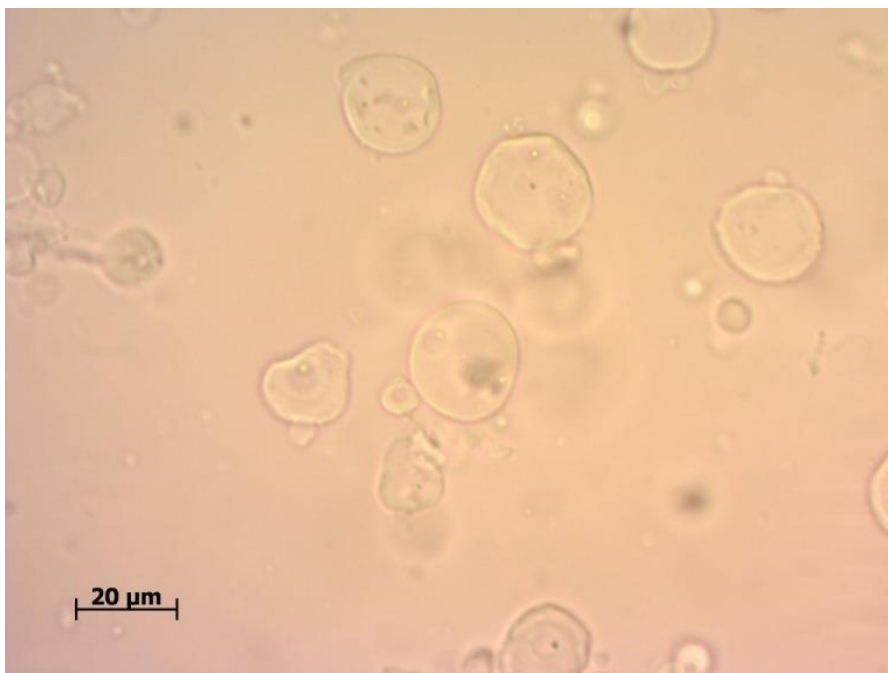


Figure 3-28 Microscope image of a sample mixture of 4.63×10^6 (0.1 g) alginate particles and 1.22×10^{11} (25 μL) chitosan particles for pH 2.3

As the alginate concentration is further increased to the level of 9.26×10^6 (0.2 g), the particles continue to remain in the dispersed phase (Figure 3-29). The dispersed phase continues to the next level of alginate. Figure 3-30 shows that the particles stay dispersed for the alginate level of 1.85×10^7 (0.4 g). These two points correspond to the dispersed uncoated phase.

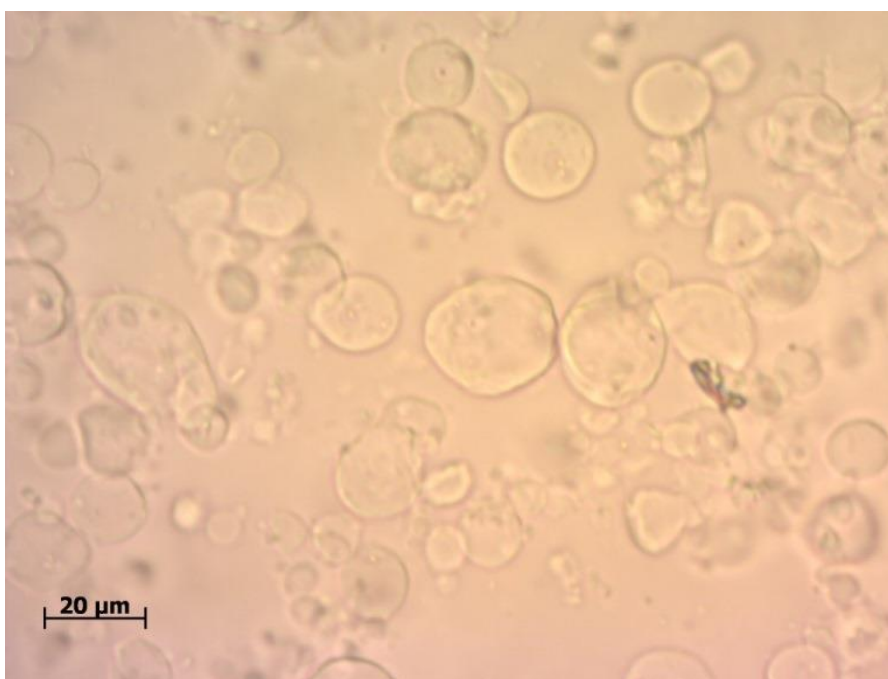


Figure 3-29 Microscope image of a sample mixture of 9.26×10^6 (0.2 g) alginate particles and 1.22×10^{11} (25 μ L) chitosan particles for pH 2.3

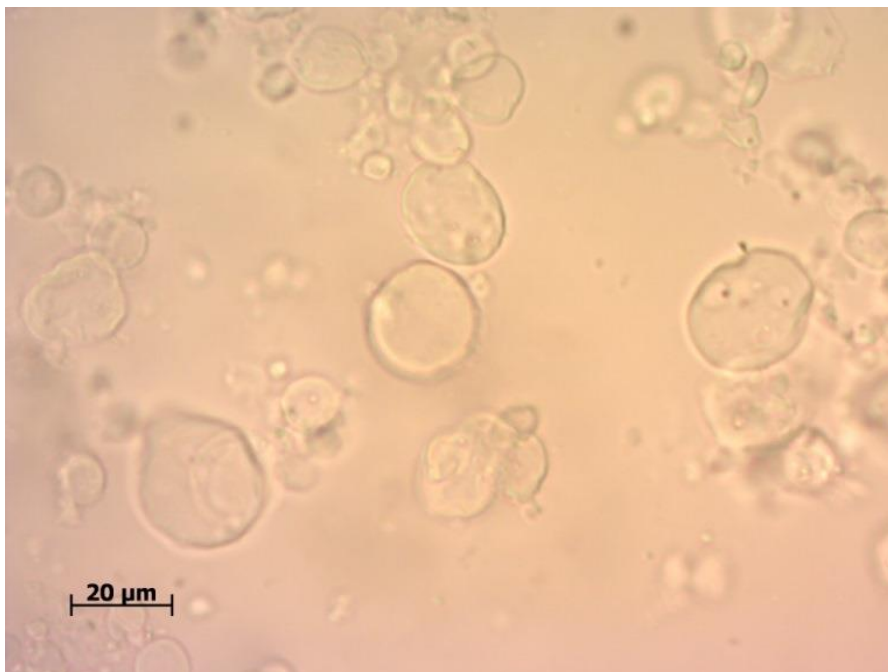


Figure 3-30 Microscope image of a sample mixture of 1.85×10^7 (0.4 g) alginate particles and 1.22×10^{11} (25 μ L) chitosan particles for pH 2.3

3.2.2 Fluorescence Spectroscopy

For each spectrum generated for samples with pH 2.3, the maximum intensity was obtained. The intensity values were averaged over three trials and plotted against the ratio of alginate to chitosan particles (Figure 3-31).

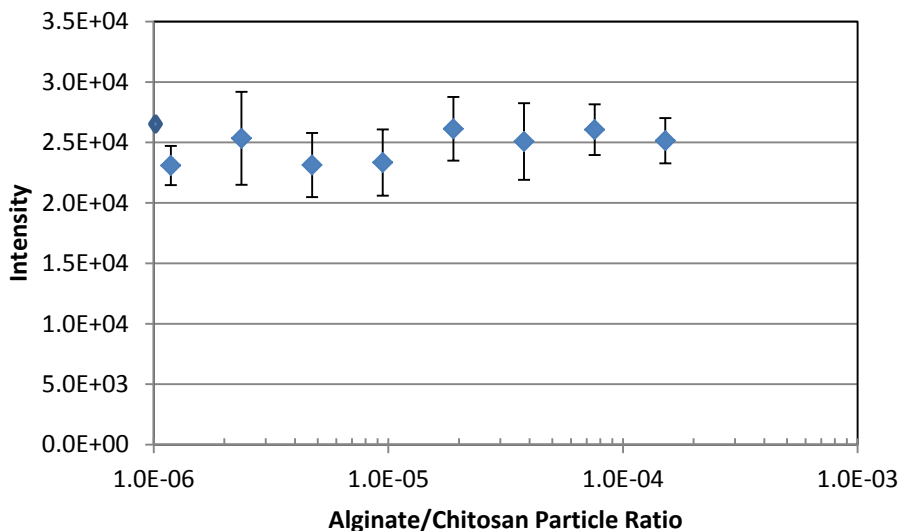


Figure 3-31 Average maximum intensity plotted against alginate/chitosan particle ratio for pH 2.3

From Figure 3-31, it can be clearly observed that the intensity doesn't vary much with increasing particle ratio. It shows nearly constant behavior. There is no clear indication of any transition between different regimes. From this graph, it is clear that the particles are in the dispersed phase. This result is similar to that obtained from microscope imaging, where dispersed coated and dispersed uncoated phases are observed.

3.2.3 Fluorescence Anisotropy

Fluorescence anisotropy was performed for the samples with pH 2.3 over the same concentration range of alginate as that of the standard sample (no HCl added) case. Sample with pH 2.3 and no alginate was used as a reference for the anisotropy measurements. Figure 3-32 shows anisotropy values averaged over three trials.

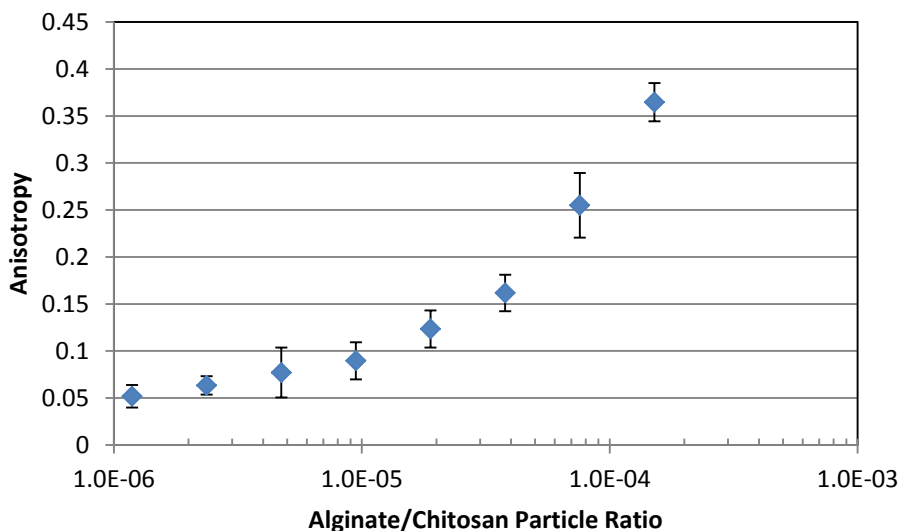


Figure 3-32 Average anisotropy values plotted against the alginate/chitosan particle ratio

The observed trend in the anisotropy values for pH 2.3 is similar to that of the standard samples (no HCl case). The anisotropy values are lower for the lower levels of alginate. As the alginate amount increases, anisotropy goes on increasing, displaying highest value for the highest amount of the alginate. One thing to note here is that, the initial values of the anisotropy for pH 2.3 are higher than that of the standard samples (no HCl case). The higher values of anisotropy at higher concentrations of alginate can be attributed to increased viscosity. The effect of viscosity and pH on the anisotropy will be discussed in a later section. The anisotropy results suggest that there may be some association between chitosan and alginate particles present in the system, though any clear regime

boundaries cannot be observed from the figure. This result is different than that of the fluorescence intensity results, where no regime change is observed.

To compare anisotropy results with the fluorescence spectroscopy results, both the anisotropy and normalized intensities were plotted against the ratio of alginate and chitosan particles. (Figure 3-33)

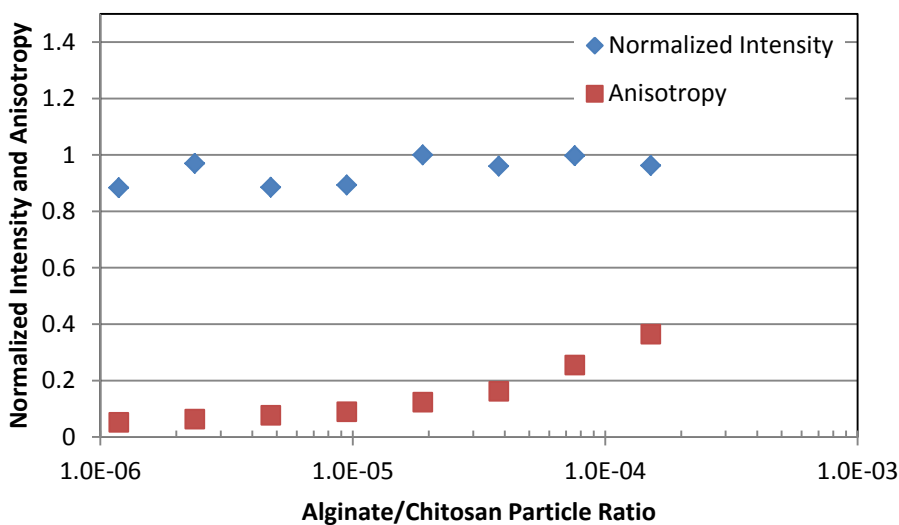


Figure 3-33 Average anisotropy and normalized intensity values plotted against the alginate /chitosan particle ratio

Here again, the results can be explained in terms of rotational diffusion and rigidity of the fluorophore environment. As explained earlier, the anisotropy is high when there is restriction to the rotational movement of the fluorophore. In case of pH 2.3, the microscope images show dispersed particles at all alginate concentrations. There are several factors which may have an effect on the way the

alginate particles interact with the chitosan particles. One of the main factors is the mechanism by which fluorophore behavior is affected in an acidic environment. The fluorescence properties of fluorescein dramatically change in a low pH environment. Free fluorescein has a pKa value of 6.5 and at low pH it shifts to the protonated form, which is poorly fluorescent. This explains why the observed values of the intensities in case of pH 2.3 are significantly lower than those observed in standard samples (no HCl case). Another reason for the observed increase in anisotropy might be steric hindrance caused by alginate particles resulting in the restricted movement. Also chitosan at low pH gets protonated resulting in chain repulsion which might cause steric hindrance resulting in the increased anisotropy. However, from anisotropy and spectroscopy results, one cannot clearly draw any definite conclusions and there might be several reasons as to why we got such results.

3.3 Results for pH 7

3.3.1 Microscope imaging

Samples with pH 7 were observed under the microscope to see the different phases or interaction regimes. The first three levels of alginate tested showed clear dispersion with distinct particles in the solution. The Figure 3-34, Figure 3-35, and Figure 3-36 show microscope images for the 1.45×10^5 (0.003125 g), 2.89×10^5 (0.00625 g) and 5.78×10^5 (0.0125 g) of the alginate particles respectively.



Figure 3-34 Microscope image of a sample mixture of 1.45×10^5 (0.003125 g) alginate particles and 1.22×10^{11} (25 μL) chitosan particles for pH 7



Figure 3-35 Microscope image of a sample mixture of 2.89×10^5 (0.00625 g) alginate particles and 1.22×10^{11} (25 μL) chitosan particles for pH 7

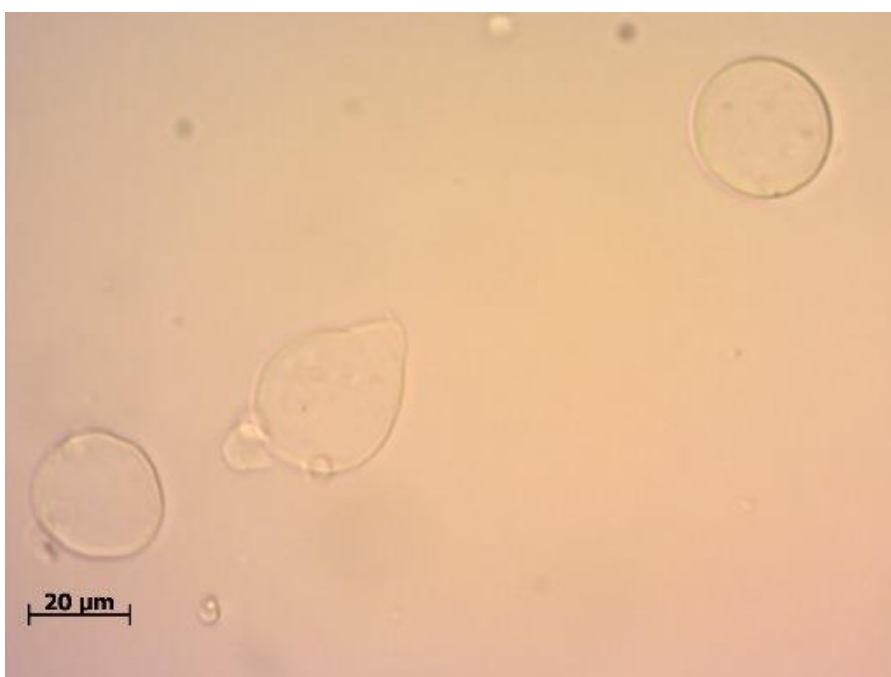


Figure 3-36 Microscope image of a sample mixture of 5.78×10^5 (0.0125 g) alginate particles and 1.22×10^{11} (25 μL) chitosan particles for pH 7

When the alginate concentration is increased further, the particles continue to stay in the dispersed phase. Figure 3-37 shows microscope image for 1.16×10^6 (0.025 g) alginate. Here we can see little assemblies of the particles which appear like an aggregate. Other than that it is mostly in the dispersed phase.



Figure 3-37 Microscope image of a sample mixture of 1.16×10^6 (0.025 g) alginate particles and 1.22×10^{11} (25 μL) chitosan particles for pH 7

The dispersed phase continues through the next levels of alginate, that is, from 2.31×10^6 (0.05 g) alginate particles to 1.85×10^7 (0.4 g) alginate particles. These four concentrations correspond to dispersed phase.

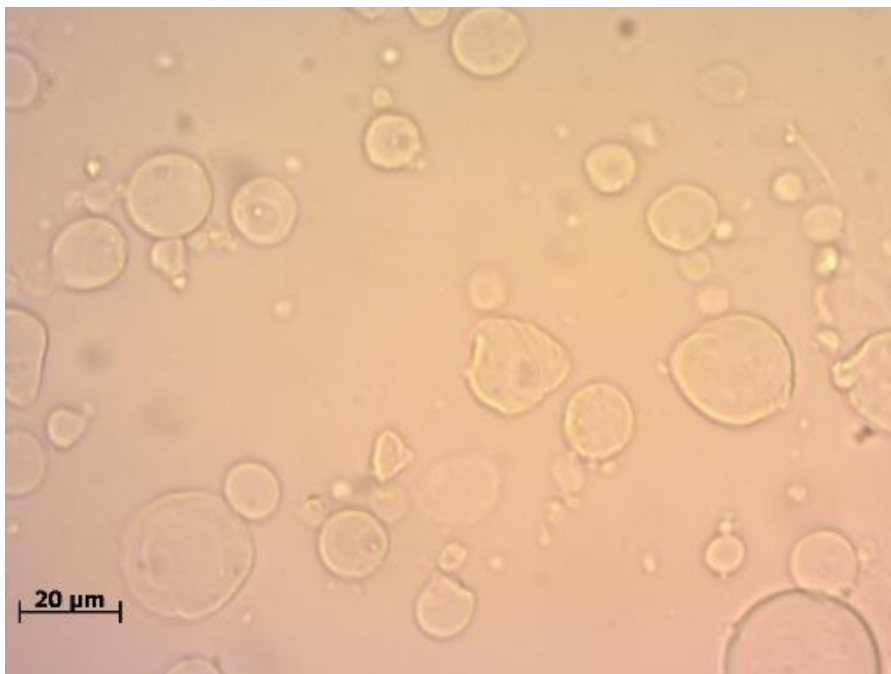


Figure 3-38 Microscope image of a sample mixture of 2.31×10^6 (0.05 g) alginate particles and 1.22×10^{11} (25 μL) chitosan particles for pH 7



Figure 3-39 Microscope image of a sample mixture of 4.63×10^6 (0.1 g) alginate particles and 1.22×10^{11} (25 μL) chitosan particles for pH 7

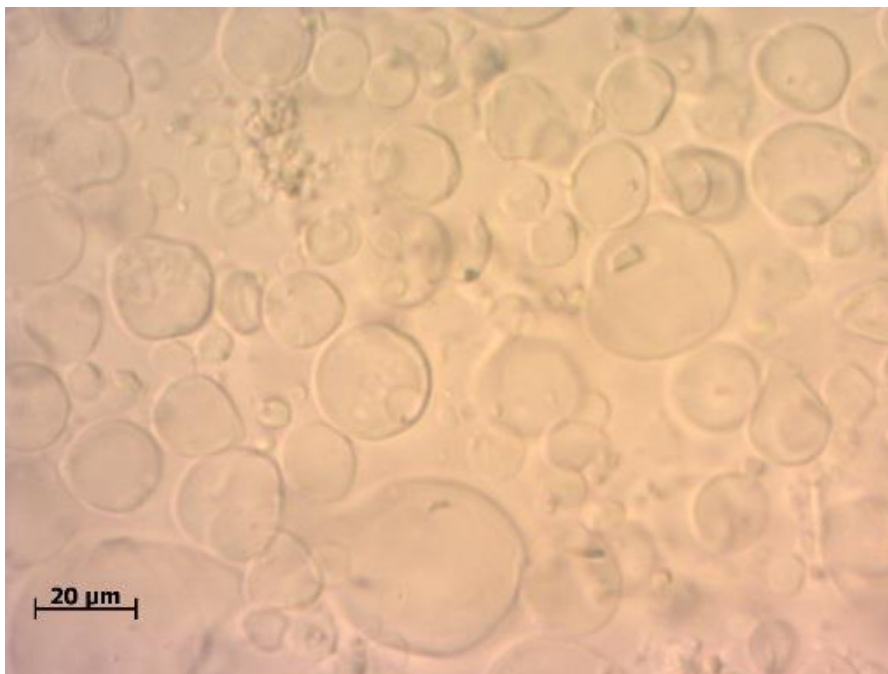


Figure 3-40 Microscope image of a sample mixture of 9.26×10^6 (0.2 g) alginate particles and 1.22×10^{11} (25 μL) chitosan particles for pH 7



Figure 3-41 Microscope image of a sample mixture of 1.85×10^7 (0.4 g) alginate particles and 1.22×10^{11} (25 μL) chitosan particles for pH 7

Here again, there is no apparent regime transition and the particles are clearly in the dispersed phase.

3.3.2 Fluorescence spectroscopy

For the samples with pH 7, maximum intensity values were obtained for each spectrum. These maximum intensity values were averaged over three trials and plotted against the ratio of the alginate and the chitosan particles.

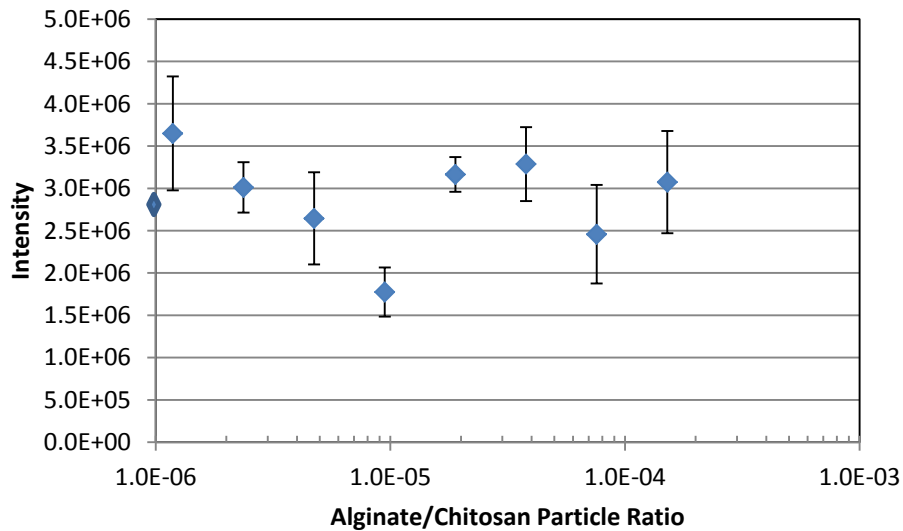


Figure 3-42 Average maximum intensity plotted against alginate/chitosan particles

As observed from the Figure 3-42, there is a lot of variability in the maximum intensity values. There is not a clear trend in the intensity with increasing ratio of alginate and chitosan particles, except perhaps at the lowest concentrations, where a continuous decrease in the intensity is observed. The

intensity values are generally quite high, as fluorescein has higher fluorescence at higher pH. As the fluorescence spectroscopy did not give clear trend, fluorescence anisotropy was performed to get better understanding of the interaction.

3.3.3 Fluorescence Anisotropy

Fluorescence anisotropy measurements were performed for the samples with pH 7. Figure 3-43 shows the variation in anisotropy values with respect to the ratio of alginate and chitosan particles.

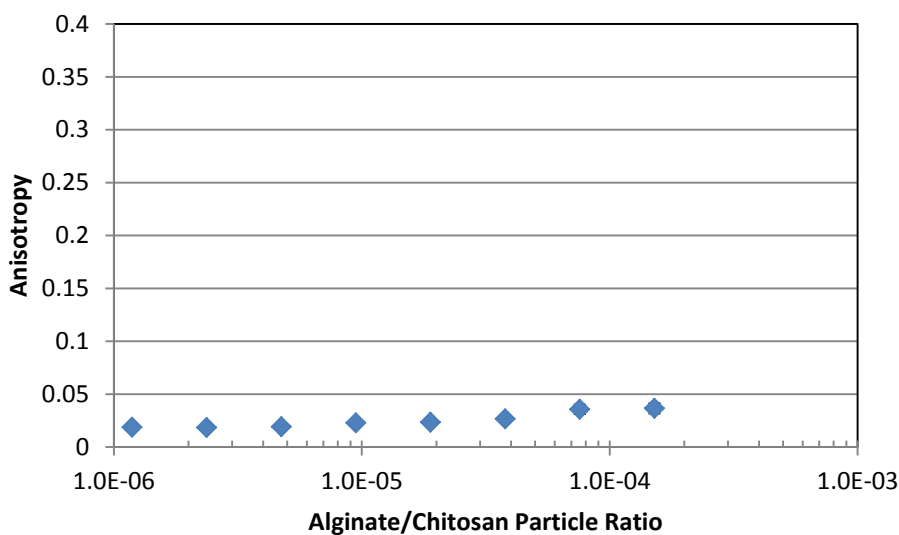


Figure 3-43 Anisotropy for pH 7 plotted against alginate/chitosan particle ratio

It can be clearly seen from the figure that the anisotropy values are near zero and do not change much with the increase in the particle ratio. As alginate is highly charged at pH 7.0, it swells and the structure becomes loose. This results in less rigid environments where chitosan particles are free to move. Hence the

anisotropy values are very low. Thus, for pH 7.0, both intensity and anisotropy measurements do not provide as clear indications of the interaction regimes as they do at other pH values.

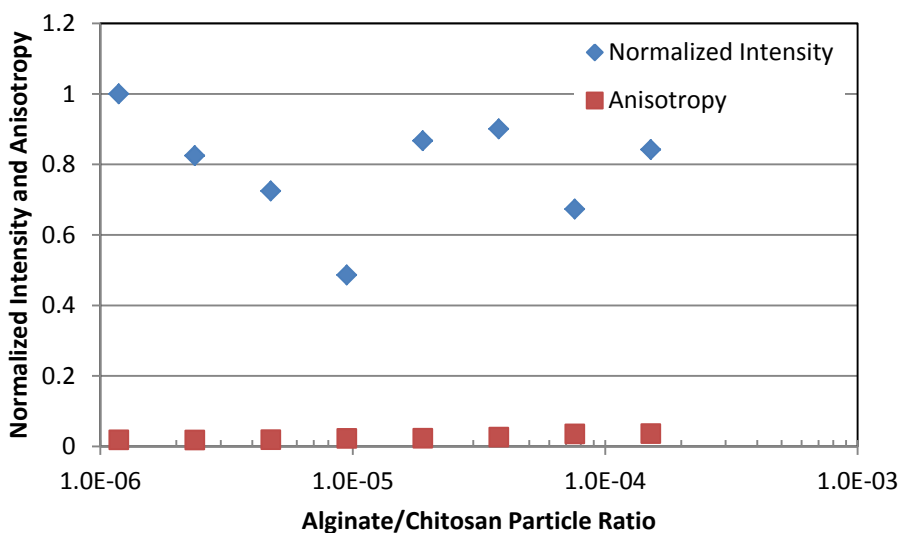


Figure 3-44 Average anisotropy and normalized intensity values plotted against the alginate /chitosan particle ratio

3.4 Comparison of Fluorescence Anisotropy and Intensity among the three pH Systems

To better understand the anisotropy results and determine the mechanisms behind the results, anisotropy values for all the three cases are plotted on the same graph.

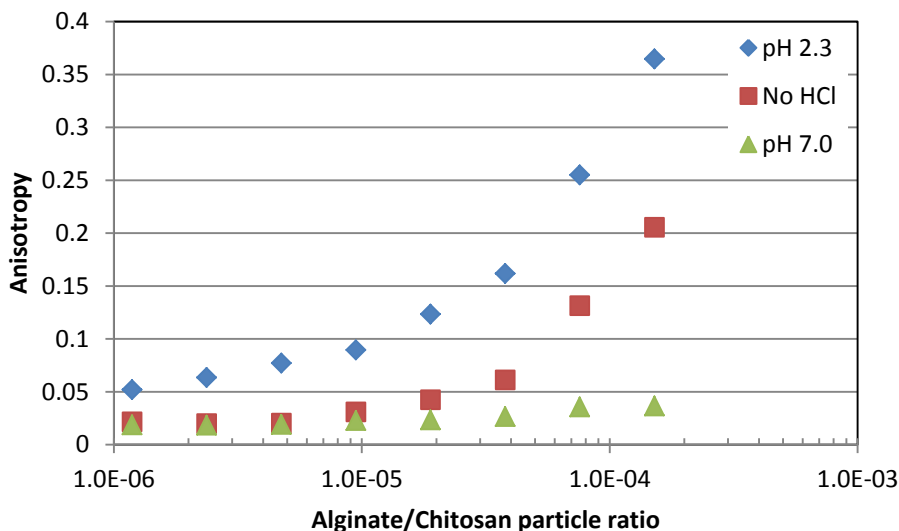


Figure 3-45 Anisotropy values for pH 2.3, No HCl and pH 7.0 samples plotted against the alginate/chitosan particle ratio

The alginate and chitosan, both being pH sensitive, behave differently in different pH environments. At lower pH values, such as pH 2.3, the environment is strongly acidic which is well below the pKa value of chitosan (6.5). At such low pH, chitosan has high positive charge which leads to the protonation of chitosan chains. These chains repel each other leading them to move as far apart as possible from each other. Due to these repulsions, chitosan chains have lower mobility as compared to that in the standard sample environment. As the fluorophore is attached to the chitosan, it becomes less mobile which results in the increased anisotropy values even at the lowest alginate/chitosan ratios.

In an acidic environment, the viscosity of the alginate solution increases due to the lower solubility of free acid [63]. pH 2.3 is below the pKa value of alginate (3.5), so that alginate polymer chains are only weakly charged at pH 2.3 and accordingly alginate hydrogel particles tend to shrink and effectively form a

denser network of cross-links, which can lead to an apparently higher viscosity environment. As mentioned earlier, anisotropy values are high when viscosity increases. Hence it can be argued that, for pH 2.3, as alginate concentration increases, the viscosity also increases to some extent resulting in the higher anisotropy values. At lower concentrations of alginate, swelling of chitosan and thereby increasing repulsion between the chains is mainly responsible for higher anisotropy values than that of the standard samples (no HCl) and pH 7.0 samples.

At higher pH, such as pH 7.0, alginate is strongly negatively charged leading to swelling of alginate particles. Due to swelling, the structure of alginate becomes loose and less rigid. Chitosan is too weakly charged at this pH to cause any significant changes in the behavior of the system. Due to this reduced rigidity in both the alginate and the chitosan particles, the fluorophores on the tagged chitosan nanoparticles are highly mobile and the observed anisotropy values are lower and near zero.

To validate the argument, the percent dissociation was calculated for each case using the Henderson-Hasselbalch equation. The obtained values are summarized in Table 2.

Table 2 Values of percentage dissociation and protonation for all the three cases

	Chitosan	Alginate
pH	% protonated	% Dissociated
2.3	99.99	5.93
5	96.93	96.93
7	24.02	99.96

From these calculations, it is clear that at lower pH, chitosan is highly protonated leading to chain repulsion. At higher pH, alginate is completely dissociated leading to high negative charge and loose structure. At intermediate pH, both chitosan and alginate are ionized, and equally contribute to the interactions.

Another possible explanation can be given in terms of ordering of chitosan particles. For pH 2.3 chitosan will be highly charged leading to a highly ordered structure which can be rigid, leading to higher anisotropy values. For standard samples, the ordering effect is present to a lesser extent. In case of pH 7.0, chitosan is only slightly charged and at the same time chitosan chains should be much more flexible leading to more mobility of the fluorophore which gives lower anisotropy values. H-bonding and hydrophobic interactions can also affect the anisotropy values of the samples [30].

Next, fluorescence spectroscopy results for each case are plotted on the same graph.

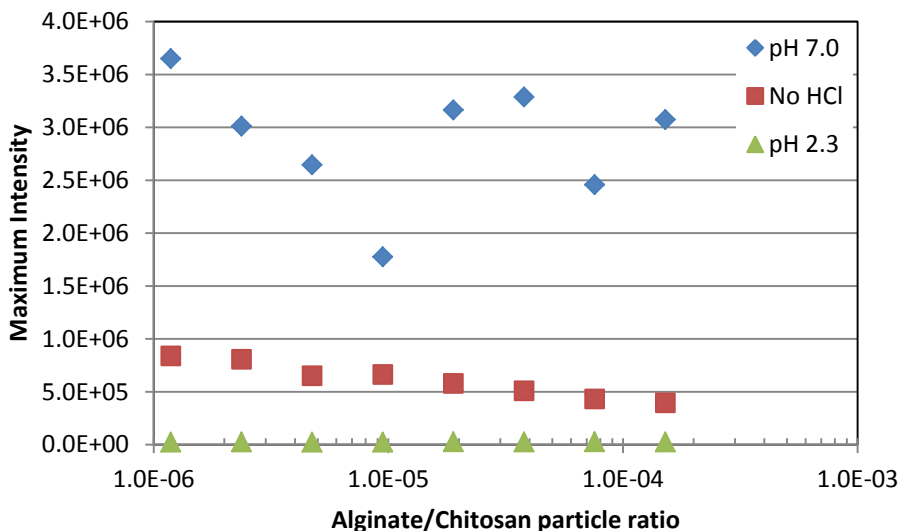


Figure 3-46 Average maximum intensity values for pH 2.3, no HCl and pH 7.0 plotted against the alginate/chitosan particle ratio

From Figure 3-46, the decreasing trend for the standard sample (no HCl) case at all concentrations of alginate can be clearly observed. The decreasing trend is also present for the pH 7.0 case at lower concentrations of alginate. In case of pH 2.3, the intensities are too low to observe any clear trend and the values appear to be roughly constant. From the results obtained, it is clear that effects such as pH and or self-quenching can be certainly the main cause for the intensity decay. pH is known to change in the close proximity of a charged surface and the extent of it is proportional to the surface potential. Negative surface potentials induce a lower surface pH compared to the bulk pH, while positive surface potentials induce higher surface pH [59]. Hence, for the pH 7.0 case, alginate is negatively charged inducing lower pH than 7.0. As fluorescence intensity goes down with pH, the decay can be observed at the dilute, lower

concentrations of alginate. For higher concentrations of alginate, several mechanisms might be working together and we do not see the decay in the intensity.

For the standard sample (no HCl) case, factors such as local pH and self-quenching are both dominant and there is a corresponding decay in the intensity at all the concentrations of alginate.

Another possible reason for the observed intensity decay can be possible electric field effects on the fluorophore [64]. For standard samples, both alginate and chitosan are highly charged. When they are in close proximity, there can be very high values of local electric fields, that is, large changes in the potential. This effect can lead to reduced fluorescence intensity. The electric field effects would be stronger for the dispersed uncoated than for the dispersed coated phase as all the chitosan particles are adjacent to the alginate surface, whereas for the dispersed coated phase, there may be multiple layers of chitosan. Thus we would expect to see lower intensity signals for the dispersed uncoated regime. In case of the pH 2.3 and pH 7.0, only one of the particles is charged leading to lower electric field impacts. This situation could explain the absence of continuous decay in the pH study results.

3.5 Results for ionic strength studies

To further understand how the interaction of alginate and chitosan particles changes when the ionic strength of the solution is changed, fluorescence

spectroscopy of the samples prepared in sodium chloride solutions of different molarity was performed.

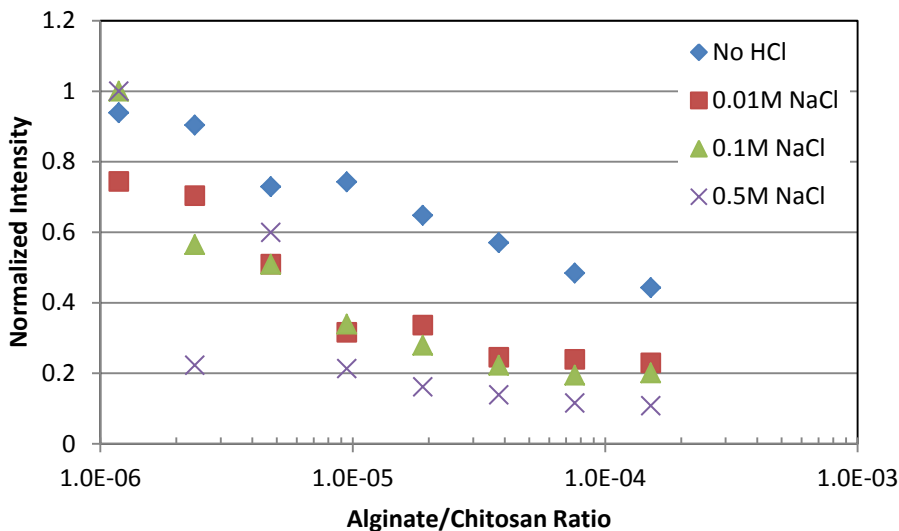


Figure 3-47 Normalized intensity plotted against alginate/chitosan particle ratio for different conditions

Figure 3-47 shows the comparison of the intensities obtained in case of the no HCl case to those obtained in solutions of different ionic strength. As observed from the figure, the intensities decrease significantly in cases of NaCl solutions, and the drop in intensity at low alginate/chitosan ratio becomes steeper as the NaCl concentration increases. The trend observed in the intensities is similar to that of the standard sample (no HCl) case and rough estimation of the regime boundaries can be made from this result. When the ionic strength of the solution is quite low, that is, 0.01 M, the regimes can be differentiated at the similar levels of the alginate particles obtained from standard sample (no HCl) studies. Further increase in the salt concentration to 0.1 M produce results similar to the 0.01 M

salt concentration. When the salt concentration is further increased to 0.5 M, there is fluctuation in the intensities for the lower levels of the alginate. However, for the rest of the alginate levels, the trend is very similar to that of the 0.01 M and 0.1 M salt concentrations.

Addition of salt results in charge shielding which in turn may reduce electrostatic repulsion between the particles. This reduced repulsion causes particles to come closer together and the agglomerated phase is observed at lower concentrations of alginate. Another possible reason for the observed intensity decay is the quenching of FITC fluorophore by chlorine ions.

Microscope images of the samples for all the three different salt concentrations were taken and compared to spectroscopy results to make sure that the interaction regime transitions were observed with microscopy.

From Figure 3-48 and Figure 3-49 it is clear that the alginates levels of 1.45×10^5 (0.003125 g) and 2.89×10^5 (0.00625 g) were in the dispersed coated phase for ionic strength of 0.01 M.

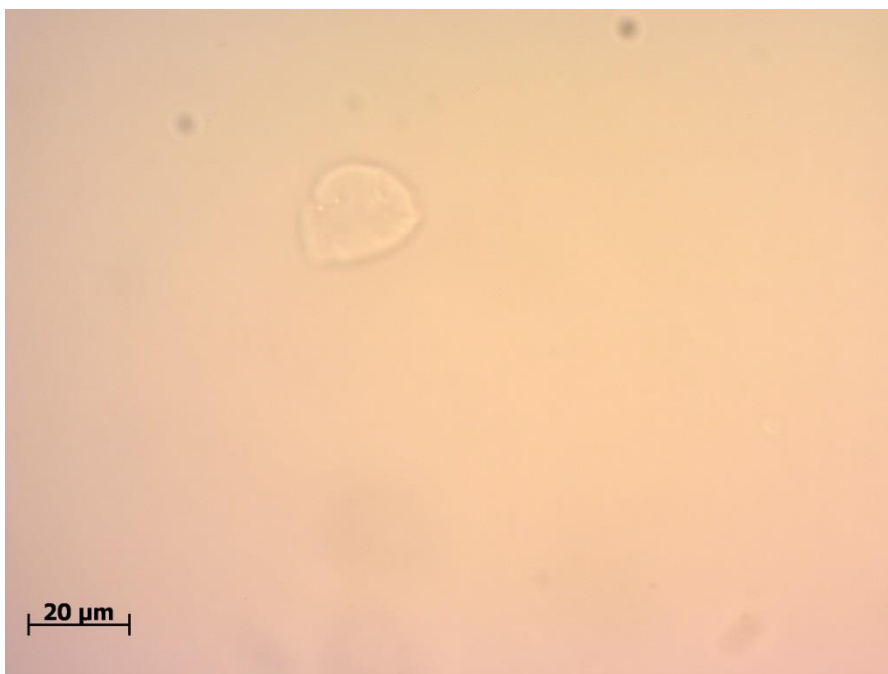


Figure 3-48 Microscope image of a sample mixture of 1.45×10^5 (0.003125 g) alginate particles and 1.22×10^{11} (25 μL) chitosan particles for 0.01 M NaCl

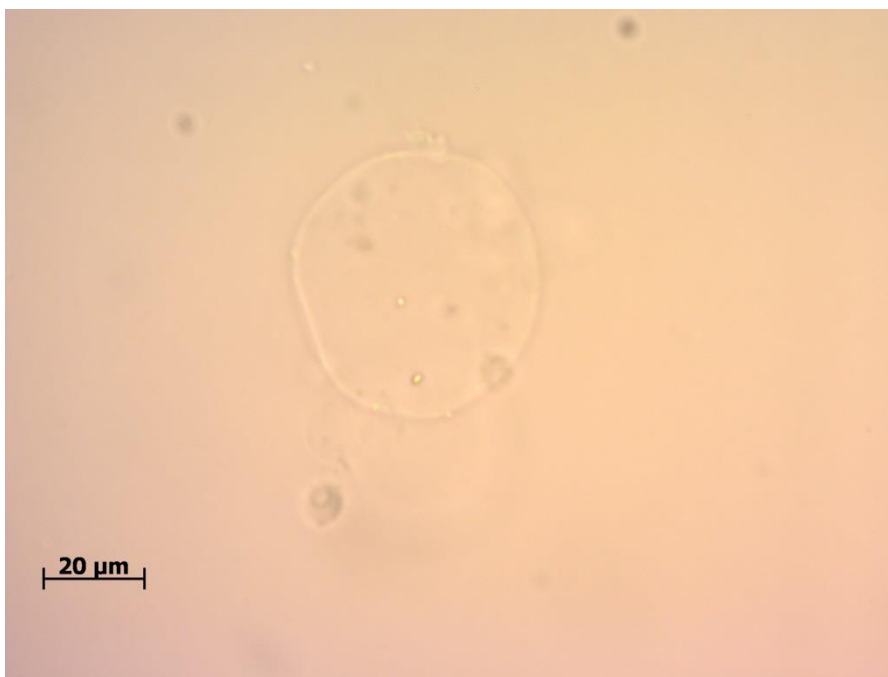


Figure 3-49 Microscope image of a sample mixture of 2.89×10^5 (0.00625 g) alginate particles and 1.22×10^{11} (25 μL) chitosan particles for 0.01 M NaCl

The alginate levels of 5.78×10^5 (0.0125 g) and 1.16×10^6 (0.025 g), both are in the agglomerated regime as seen in Figure 3-50 and Figure 3-51 respectively.



Figure 3-50 Microscope image of a sample mixture of 5.78×10^5 (0.0125 g) alginate particles and 1.22×10^{11} (25 μL) chitosan particles for 0.01 M NaCl

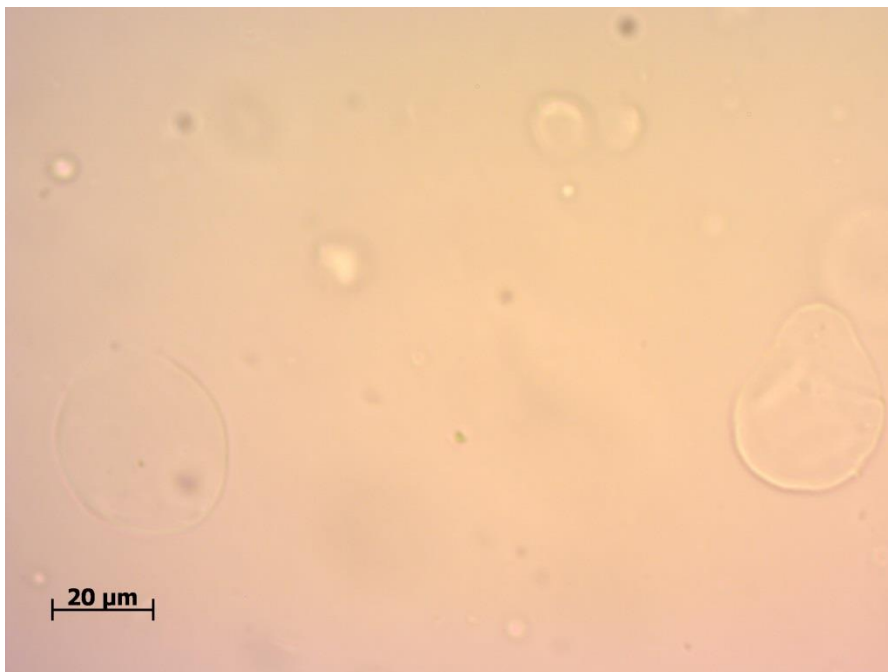


Figure 3-51 Microscope image of a sample mixture of 1.16×10^6 (0.025 g) alginate particles and 1.22×10^{11} (25 μL) chitosan particles for 0.01 M NaCl

Next four levels of alginate represent the dispersed uncoated regime. The dispersed uncoated regime continues from 2.31×10^6 (0.05 g) to 1.85×10^7 (0.4 g) alginate particles. (Figure 3-52 - Figure 3-55)

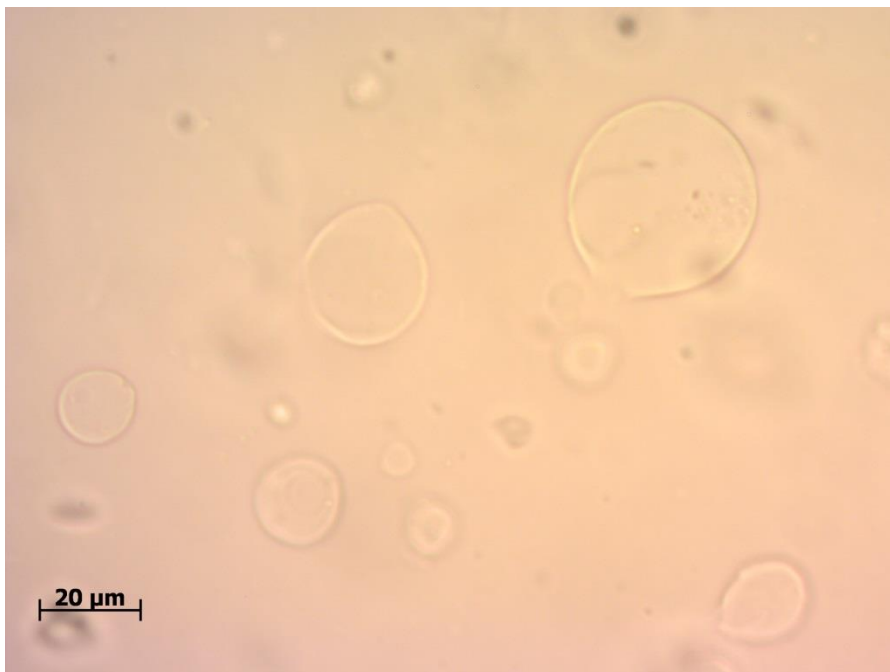


Figure 3-52 Microscope image of a sample mixture of 2.31×10^6 (0.05 g) alginate particles and 1.22×10^{11} (25 μL) chitosan particles for 0.01 M NaCl

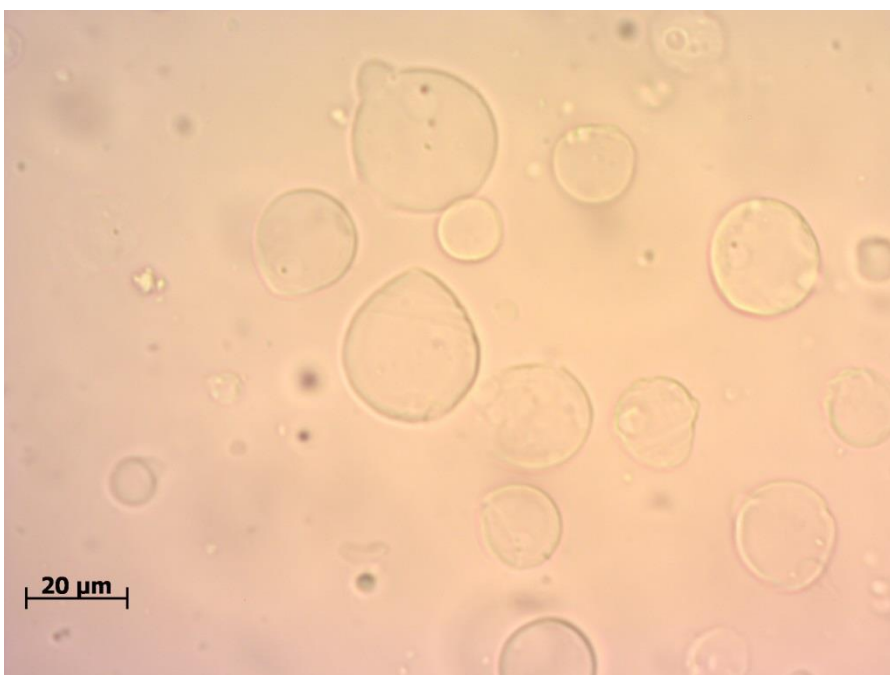


Figure 3-53 Microscope image of a sample mixture of 4.63×10^6 (0.1 g) alginate particles and 1.22×10^{11} (25 μL) chitosan particles for 0.01 M NaCl

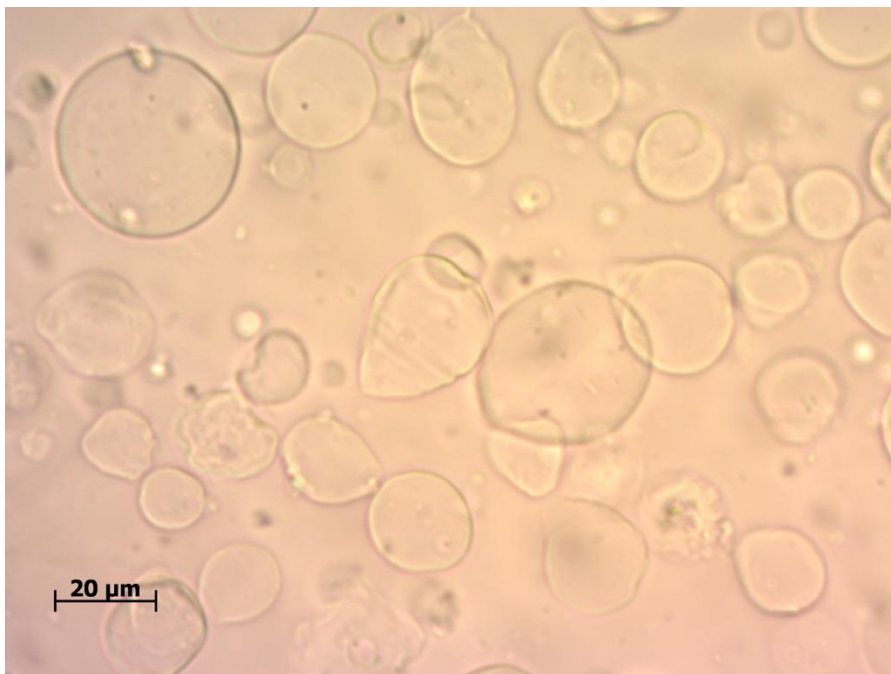


Figure 3-54 Microscope image of a sample mixture of 9.26×10^6 (0.2 g) alginate particles and 1.22×10^{11} (25 μL) chitosan particles for 0.01 M NaCl



Figure 3-55 Microscope image of a sample mixture of 1.85×10^7 (0.4 g) alginate particles and 1.22×10^{11} (25 μL) chitosan particles for 0.01 M NaCl

Microscope images for the samples with 0.1 M and 0.5 M ionic strength were taken. However, it was hard to see the particles for almost all the levels of the alginate in both the cases. Images were obtained for only higher levels of alginate. Figure 3-56 shows the image for the alginate level of 1.85×10^7 (0.4 g) for 0.1 M ionic strength.

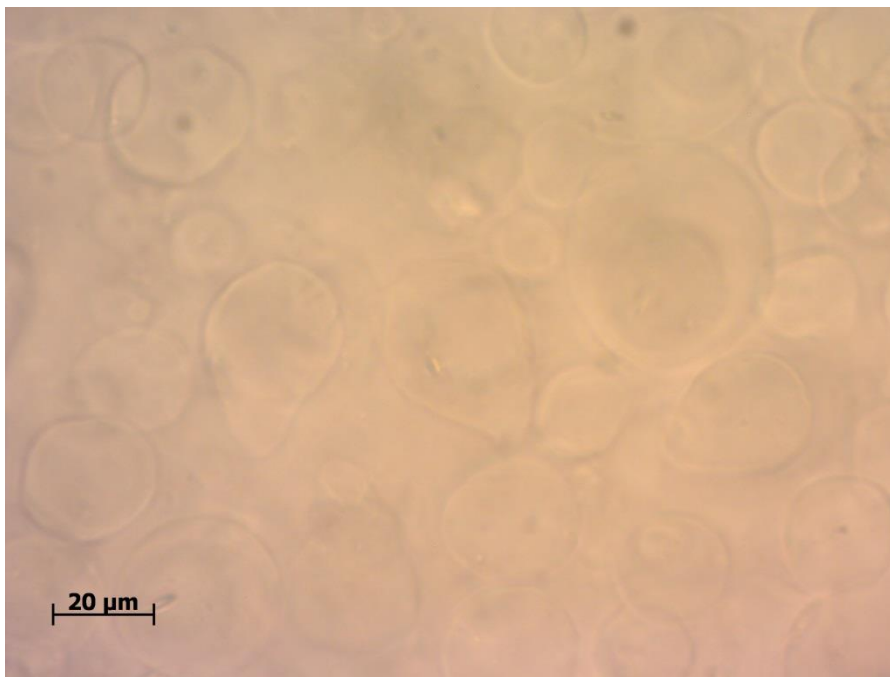


Figure 3-56 Microscope image of a sample mixture of 1.85×10^7 (0.4 g) alginate particles and 1.22×10^{11} (25 μ L) chitosan particles for 0.1 M NaCl

The image is not clear and very cloudy to make out any clear estimate of the interaction regime. Figure 3-57 shows the image for alginate level of 1.85×10^7

(0.4 g) for 0.5 M ionic strength and this image is also cloudy to make any guess about the interaction regime.

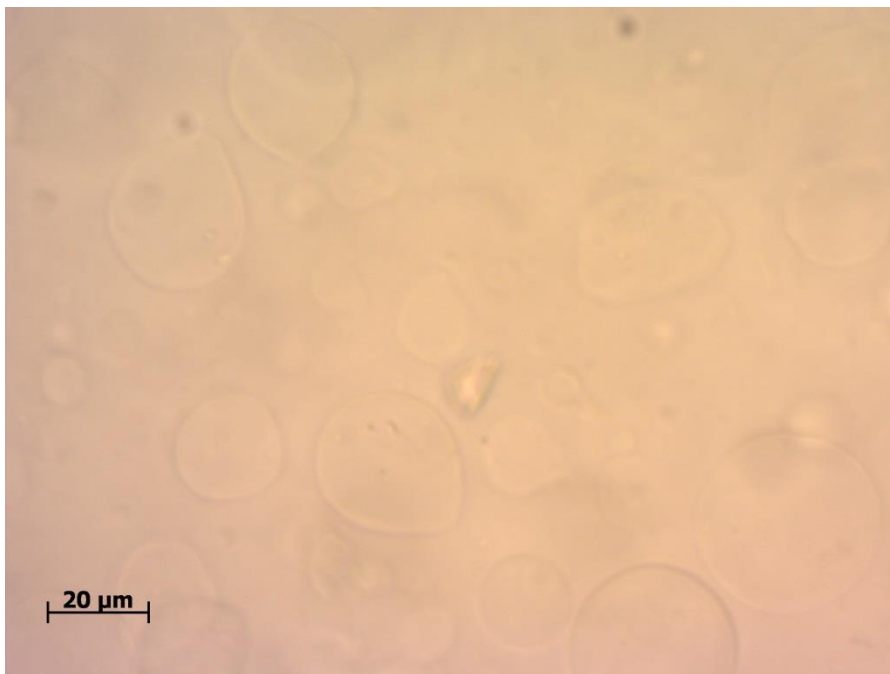


Figure 3-57 Microscope image of a sample mixture of 1.85×10^7 (0.4 g) alginate particles and 1.22×10^{11} (25 μ L) chitosan particles for 0.5 M NaCl

There might be matching of the refractive index to make the alginate particles hard to see or the alginate particles' cross-linking was disrupted. If it is the former case, then fluorescence spectroscopy results have a chance of being accurate, but if it is the latter case, then there is no chance of the spectroscopy results being accurate. Hence, except for the case of 0.01 M salt concentration, it

cannot be said definitely that the fluorescence spectroscopy provided better results than the microscopy.

3.6 *In Situ* measurements

In order to check the applicability of the fluorescence spectroscopy for *in situ* measurements, experiments using fiber optics probe were performed. The alginate levels were the same as that of the standard sample (no HCl) case. The sample is directly excited by light passing through the fiber optics probe which is in contact with the vial surface. Readings were taken for both the sample and blanks. Blank values were subtracted from sample values to get accurate intensity readings.

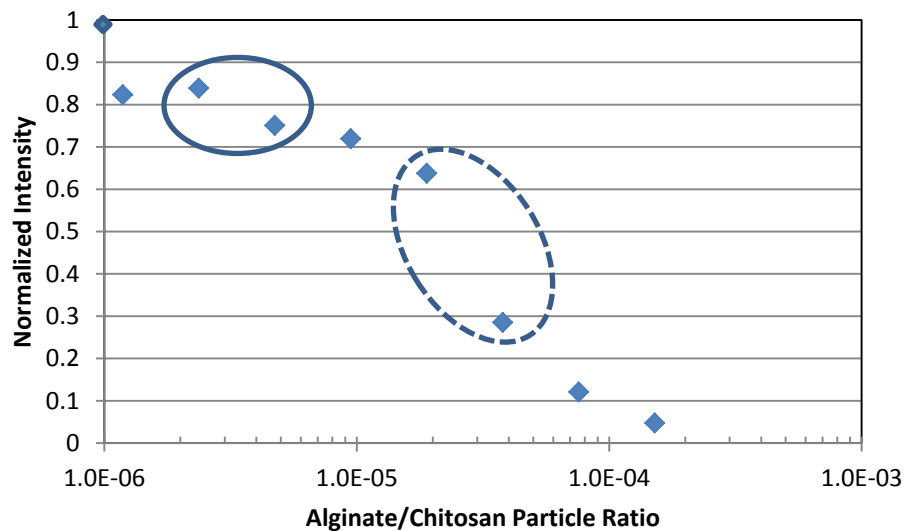


Figure 3-58 Normalized intensity plotted against the alginate/chitosan particle ratio for the *in situ* measurements

From Figure 3-58 it is clear that the trend observed from *in situ* measurements is similar to the one observed from the standard sample (no HCl) case. Here the regime transition from the agglomerated to the dispersed uncoated phase is more obvious than the one in the standard sample (no HCl) results. These results indicate distinct boundaries between the dispersed coated to agglomerated and agglomerated to the dispersed uncoated phase.

3.7 Summary

In this study, fluorescence spectroscopy coupled with fluorescence anisotropy has proven to be a viable method to determine particle interaction regimes between alginate microparticles and fluorescent chitosan nanoparticles suspended in deionized water. Initially, interaction regime boundaries were determined with optical microscope imaging for such “standard samples.” Using fluorescence spectroscopy, the regime change boundary between the dispersed coated regime and the agglomerated regime was detected, most likely due to large increases in local pH effects and possibly self-quenching as a sharply increased fraction of the tagged chitosan particles is located in close proximity to alginate particle surfaces. The boundary between the agglomerated phase and the dispersed uncoated phase was obtained from fluorescence anisotropy measurements, due to the restriction in rotation and movement when chitosan particles are near or adsorbed on the alginate particles. To gain understanding of the shifting of the interaction regime boundaries, laser diffraction particle size analysis was performed. Laser diffraction spectroscopy successfully determined the interaction regime boundaries between the dispersed coated, agglomerated

and dispersed uncoated phases. Simple particle calculations based on DLVO theory were performed in order to understand why the boundaries were observed at the particular particle ratios.

For the pH variation study, microscope images showed that the particles were dispersed for all of the concentrations of the alginate. Fluorescence spectroscopy and fluorescence anisotropy results for the pH variation study indicate that the local pH effect is likely to be the main cause of the intensity decay. The observed anisotropy values were most probably caused by changes in the local viscosity of the system.

For varying ionic strength studies, fluorescence spectroscopy indicated regime boundaries which corroborated microscope imaging results for the case of 0.01 M salt concentration. In the cases of 0.1 M and 0.5 M salt concentrations, particles were not clearly visible under the microscope, and may have been refractive index matched with the fluid. Finally, fluorescence spectroscopy measurements were acquired *in situ*. The results successfully indicated the transitions between interaction regime boundaries.

Chapter 4
CONCLUSIONS AND FUTURE WORK

4.1 Conclusions

This work has investigated interactions between hydrogel colloidal particles. Various techniques such as optical imaging, fluorescence spectroscopy, fluorescence anisotropy, and laser diffraction spectroscopy were applied to study the system. The main objective behind this study was to enhance understanding of the observed phenomena in order to better create nanoparticle coated microparticles.

First, fluorescence spectroscopy was applied to study the interaction between negatively charged alginate microparticles and positively charged chitosan nanoparticles. Optical microscopy was used to determine the interaction regime boundaries between the dispersed coated and the agglomerated and between the agglomerated and the dispersed uncoated regimes. Then, fluorescence spectroscopy was used to determine if the interaction regime boundaries can be seen in the variations of the intensity readings. It was found that the boundary between the dispersed coated and agglomerated regimes was indicated by a sharp decrease in the slope of the normalized average intensity plotted against ratio of alginate and chitosan particles. The agglomerated and dispersed uncoated regime boundary was not clearly detected. At higher concentrations of alginate, the intensity was found to have lower values due to a combination of different factors such as local pH effects and self-quenching. For better understanding of the regime change, fluorescence anisotropy measurements were performed. Anisotropy values were found to increase with the amount of alginate particles due to restriction in movement and

corresponding hindered rotation of the fluorophore. Laser diffraction particle size analysis was performed to get the particles' size in different regimes. Laser diffraction accurately provided the regime boundaries for all of the three regimes. It was found to be a suitable alternative to optical microscope imaging, not having the typical limitations of microscopy. Moreover, from simple particle calculations based on the DLVO theory, it was concluded that the surface charge neutralization and packing limitation on chitosan particles were the main mechanisms for the transition between the dispersed uncoated to agglomerated regimes and the agglomerated to dispersed coated regimes respectively.

Next, a study of the interaction regime boundaries while varying pH and ionic strength was done. This study was performed to study the effect of pH and ionic strength on interaction regime boundaries and also to test the viability of fluorescence techniques in different environments for detecting interaction regime boundaries. The fluorescence spectroscopy and anisotropy results were compared to microscope images. Results for the pH study gave clear indications that the local pH effect was likely the main mechanism for the reduction in the intensity and the viscosity effect was probably mainly responsible for the observed trends in the anisotropy values. For the case of varying ionic strength, fluorescence spectroscopy detected accurate regime boundaries matching the microscope images. For higher values of salt concentrations, though, microscopy did not provide clear images and nothing conclusive could be deduced from the fluorescence spectroscopy results.

Finally, fluorescence spectroscopy was tested as *in situ* characterization method. It accurately determined interaction regime boundaries which matched the results obtained in case of the standard samples.

4.2 Future Work

In this study, both the particles studied were hydrophilic hydrogels. For future work, fluorescence spectroscopy can be further explored by using a combination of hydrophobic and hydrophilic particles. It would be interesting to see how changing the particles affects the interactions and the effectiveness of fluorescence spectroscopy.

Alginate and chitosan particles are encapsulation agents. Assemblies containing material encapsulated by alginate and chitosan can be studied using fluorescence spectroscopy.

Use of another fluorophore for tagging and its applicability to find the regime boundaries can be studied. FITC is a toxic fluorophore and cannot be used in oral drug delivery applications. Instead, a nontoxic fluorophore can be used.

There is a need for more research on how fluorescence spectroscopy can be effectively used for the low pH conditions. This investigation would be beneficial for pH controlled drug delivery. Another factor affecting the fluorescence intensity is temperature which was not considered in this study. It can be useful to study how temperature affects the performance of fluorescence spectroscopy in determining interaction regime boundaries.

Finally, a more in depth study can be done on how fluorescence techniques can be used for on-line or *in situ* detection of aggregation or characterization.

REFERENCES

- [1] J.Th.G. Overbeek, "Interparticle forces in colloid science," *Powder Technology*, vol. 37, pp. 198-208, 1984.
- [2] A. M. Islam, B. Z. Chowdhry, and M. J. Snowden, "Heteroaggregation in colloidal dispersions," *Advances in Colloid and Interface Science*, vol. 62, pp. 109-136, 1995.
- [3] M. Bradley, A. M. Lazim, and J. Eastoe, "Stimulus-Responsive Heteroaggregation of Colloidal Dispersions: Reversible Systems and Composite Materials," *Polymer*, vol. 3, pp. 1036-1050, 2011.
- [4] V. Tohver, A. Chan, O. Sakurada, and J. A. Lewis, "Nanoparticle engineering of complex fluid behavior," *Langmuir*, vol. 17, pp. 8414-8421, 2001a.
- [5] K. Yu et al., "Copper ion adsorption by chitosan nanoparticles and alginate microparticles for water purification applications," *Colloids and Surfaces A: Physicochemical and Engineering Aspects*, vol. 425, no. 31-41, 2013.
- [6] V. Tohver, J. E. Smay, A. Braem, P. V. Braun, and J. A. Lewis, "Nanoparticle halos: A new colloid stabilization mechanism," *Proceedings of the National Academy of Sciences of the United States of America*, vol. 98, pp. 8950-8954, 2001b.
- [7] S. A. Agnihotri, N. N. Mallikarjuna, and T. M. Aminabhavi, "Recent advances on chitosan-based micro-and nanoparticles in drug delivery," *Journal of Controlled Release*, vol. 100, pp. 5-28, 2004.
- [8] K. Furusawa and O. D. Velev, "Electrokinetic behavior in synthetic process of composite particles," *Colloids and Surfaces A: Physicochemical and Engineering Aspects*, vol. 159, pp. 359-371, 1999.
- [9] A. Fernandez-Barbero, A. Loxley, and B. Vincent, "Heteroaggregation between charged hard and soft particles," *Progress in Colloid and Polymer Science*, vol. 115, pp. 84-87, 2000.
- [10] A. T. Chan and J. A. Lewis, "Electrostatically tuned interactions in silica microsphere-polystyrene nanoparticle mixtures," *Langmuir*, vol. 21, pp. 8576-8579, 2005.
- [11] J. F. Gilchrist, A. T. Chan, E. R. Weeks, and J. A. Lewis, "Phase behavior and 3d structure of strongly attractive microsphere-nanoparticle mixtures,"

- Langmuir*, vol. 21, pp. 11040-11047, 2005.
- [12] E. N. Scheer and K. S. Schweizer, "Haloing, flocculation, and bridging in colloid-nanoparticle suspensions," *Journal of Chemical Physics*, vol. 128, p. 164905, 2008.
- [13] M. N. Ravi Kumar, "A review of chitin and chitosan applications," *Reactive and functional polymers*, vol. 46, pp. 1-27, 2000.
- [14] B. F. Gibbs, S. Kermasha, I. Alli, and C. N. Mulligan, "Encapsulation in the food industry: a review," *International Journal of Food Sciences and Nutrition*, vol. 50, pp. 213-224, 1999.
- [15] H. J. Hester-Reilly and N. C. Shapley, "Imaging contrast effects in alginate microbeads containing trapped emulsion droplets," *Journal of Magnetic Resonance*, vol. 188, pp. 168-175, 2007.
- [16] J. Berger et al., "Structure and interactions in covalently and ionically crosslinked chitosan hydrogels for biomedical applications," *European Journal of Pharmaceutics and Biopharmaceutics*, vol. 57, pp. 19-34, 2004.
- [17] P. R. Rege, D. J. Shukla, and L. H. Block, "Chitinosans as tableting excipients for modified release delivery systems," *International Journal of Pharmaceutics*, vol. 181, pp. 49-60, 1999.
- [18] M. L. Duarte, M. C. Ferreira, M. R. Marvão, and J. Rocha, "An optimized method to determine the degree of acetylation of chitin and chitosan by FTIR spectroscopy," *International Journal of Biological Macromolecules*, vol. 31, pp. 1-8, 2002.
- [19] S. Sabnis and L. H. Block, "Chitosan as an enabling excipient for drug delivery systems: I. Molecular modifications," *International Journal of Biological Macromolecules*, vol. 27, pp. 181-186, 2000.
- [20] F. L. Mi et al., "Chitosan-polyelectrolyte Complexation for the Preparation of Gel Beads and Controlled Release of Anticancer Drug. I. Effect of Phosphorous Polyelectrolyte Complex and Enzymatic Hydrolysis of Polymer," *Journal of Applied Polymer Science*, vol. 74, pp. 1868-1879, 1999.
- [21] P. M. Claesson and B. W. Ninham, "pH-dependent interactions between adsorbed chitosan layers," *Langmuir*, vol. 8, pp. 1406-1412, 1992.

- [22] Y. X. Xu, K. M. Kim, M. A. Hanna, and D. Nag, "Chitosan–starch composite film: preparation and characterization," *Industrial Crops and Products*, vol. 21, pp. 185-192, 2005.
- [23] V. Dodane and V. D. Vilivalam, "Pharmaceutical applications of chitosan," *Pharmaceutical Science & Technology Today*, vol. 1, pp. 246-253, 1998.
- [24] W. Paul and C. Sharma, "Chitosan, a drug carrier for the 21st century: a review," *STP pharma sciences*, vol. 10, pp. 5-22, 2000.
- [25] F. Shahidi, J. K. V. Arachchi, and Y. J. Jeon, "Food applications of chitin and chitosans," *Trends in food science & technology*, vol. 10, pp. 37-51, 1999.
- [26] V. Sinha et al., "Chitosan microspheres as a potential carrier for drugs," *International Journal of Pharmaceutics*, vol. 274, pp. 1-33, 2004.
- [27] T. Banerjee, S. Mitra, A. Kumar Singh, R. Kumar Sharma, and A. Maitra, "Preparation, characterization and biodistribution of ultrafine chitosan nanoparticles," *International Journal of Pharmaceutics*, vol. 243, pp. 93-106, 2002.
- [28] L. L. Li et al., "Magnetic and fluorescent multifunctional chitosan nanoparticles as a smart drug delivery system," *Nanotechnology*, vol. 18, p. 405102, 2007.
- [29] J. Zhi, Y. J. Wang, and G. S. Luo, "Adsorption of diuretic furosemide onto chitosan nanoparticles prepared with a water-in-oil nanoemulsion system," *Reactive and Functional Polymers*, vol. 65, pp. 249-257, 2005.
- [30] R. B. Qaqish and M. M. Amiji, "Synthesis of a fluorescent chitosan derivative and its application for the study of chitosan-mucin interactions," *Carbohydrate Polymers*, vol. 38, pp. 99-107, 1999.
- [31] G. Klöck et al., "Biocompatibility of mannuronic acid-rich alginates," *Biomaterials*, vol. 18, pp. 707-713, 1997.
- [32] F. L. Mi, H. W. Sung, and S. S. Shyu, "Drug release from chitosan–alginate complex beads reinforced by a naturally occurring cross-linking agent," *Carbohydrate Polymers*, vol. 48, pp. 61-72, 2002.
- [33] H. L. Lai, A. Abu'Khalil, and D. Q. Craig, "The preparation and characterization of drug-loaded alginate and chitosan sponges,"

International journal of Pharmaceutics, vol. 251, pp. 175-181, 2003.

- [34] S. T. Moe, K. I. Dragel, and O. Smidsrød, "Alginates," in *Food Polysaccharides and Their Applications*, Stephen AM, Ed.
- [35] A. Steinbüchel and S. K. Rhee, *Polysaccharides and polyamides in the food industry: properties, production, and patents.*: Wiley-VCH Verlag GmbH & CO. KGaA, 2005.
- [36] H. H. Tønnesen and J. Karlsen, "Alginate in drug delivery systems," *Drug development and industrial pharmacy*, vol. 28, pp. 621-630, 2002.
- [37] S. Takka and F. Acartürk, "Calcium alginate microparticles for oral administration: Iii. The effect of crosslink agents and various additive polymers on drug release and drug entrapment efficiency," *Pharmazie*, vol. 54, pp. 137-139, 1999b.
- [38] M. George and T. E. Abraham, "Polyionic hydrocolloids for the intestinal delivery of protein drugs: Alginate and chitosan- a review," *Journal of Controlled Release*, vol. 114, pp. 1-14, 2006.
- [39] J. R. Lakowicz, *Principles of fluorescence spectroscopy.*: Springer, 2007.
- [40] I. D. Johnson, *The molecular probes handbook: A guide to fluorescent probes and labeling technologies.*: Life Technologies Corporation, 2010.
- [41] J. R. Albani, *Principles and applications of fluorescence spectroscopy.*: John Wiley & Sons, 2008.
- [42] G. M. Strasburg and R. D. Ludescher, "Theory and applications of fluorescence spectroscopy in food research," *Trends in Food Science & Technology*, vol. 6, pp. 69-75, 1995.
- [43] A. B. Moreira, I. L. Dias, G. O. Neto, E. A. Zagatto, and L. T. Kubota, "Solid-phase fluorescence spectroscopy for the determination of acetylsalicylic acid in powdered pharmaceutical samples," *Analytica chimica acta*, vol. 523, pp. 49-52, 2004.
- [44] K., Lippard, S., Vassiliades, G., Bauer, W. Jennette, "Metallointercalation reagents. 2-hydroxyethanethiolato (2, 2', 2''-terpyridine)-platinum (ii) monocation binds strongly to DNA by intercalation.," *Proceedings of the National Academy of Sciences*, vol. 71, pp. 3839-3843, 1974.

- [45] A. Gong, X. Zhu, Y. Hu, and S. Yu, "A fluorescence spectroscopic study of the interaction between epristeride and bovin serum albumine and its analytical application," *Talanta*, vol. 73, pp. 668-673, 2007.
- [46] T. Nam et al., "Tumor targeting chitosan nanoparticles for dualmodality optical/MR cancer imaging," *Bioconjugate chemistry*, vol. 21, pp. 578-582, 2010.
- [47] K. V. Deshpande, "Particulate flows and heteroaggregation studied by optical imaging and fluorescence spectroscopy," Rutgers, The State University of New Jersey, New Brunswick, US, Ph.D. Thesis 2014.
- [48] W. B. Dandliker and G. A. Feigen, "Quantification of the antigen-antibody reaction by the polarization of fluorescence," *Biophysical and biochemical research communications*, vol. 5, pp. 299-304, 1961.
- [49] T. Hayashi, Y. Ishizaki, M. Michihata, Y. Takaya, and S. I. Tanaka, "Nanoparticle sizing method based on fluorescence anisotropy analysis," *Measurement*, vol. 59, pp. 382-388, 2015.
- [50] M. Sowmiya, A. K. Tiwari, and S. K. Saha, "Fluorescent probe studies of micropolarity, premicellar and micellar aggregation of non-ionic Brij surfactants," *Journal of colloid and interface science*, vol. 344, pp. 97-104, 2010.
- [51] G. B. de Boer, C. de Weerd, D. Thoenes, and H. W. Goossens, "Laser diffraction spectrometry: Fraunhofer diffraction versus Mie scattering," *Particle & Particle Systems Characterization*, vol. 4, pp. 14-19, 1987.
- [52] M. Huang, E. khor, and L. Y. Lim, "Uptake and cytotoxicity of chitosan molecules and nanoparticles: effects of molecular weight and degree of deacetylation," *Pharmaceutical research*, vol. 21, pp. 344-353, 2004.
- [53] M. Torres-Lugo and N. A. Peppas, "Molecular design and in vitro studies of novel pH-sensitive hydrogels for the oral delivery of calcitonin," *Macromolecules*, vol. 32, pp. 6646-6651, 1999.
- [54] K. Y. Lee and D. J. Mooney, "Hydrogels for tissue engineering," *Chemical reviews*, vol. 101, pp. 1869-1880, 2001.
- [55] J. D. Ehrick et al., "Glucose responsive hydrogel networks based on protein recognition," *Macromolecular bioscience*, vol. 9, pp. 864-868, 2009.

- [56] R. Yoshida et al., "Comb-type grafted hydrogels with rapid deswelling response to temperature changes," *Nature*, vol. 374, pp. 240-242, 1995.
- [57] G. S. Lango, M. Olvera de la Cruz, and I. Szleifer, "pH-Controlled Nanoaggregation in Amphiphilic Polymer Co-networks," *ACS nano*, vol. 7, pp. 2693-2704, 2013.
- [58] B. Zhao and J. S. Moore, "Fast pH-and ionic strength-responsive hydrogels in microchannels," *Langmuir*, vol. 17, pp. 4758-4763, 2001.
- [59] S. Moreno-Flores et al., "Physical attachment of fluorescent protein particles to atomic force microscopy probes in aqueous media: Implications for surface pH, fluorescence, and mechanical properties studies," *Microscopy Research and Technique*, vol. 73, pp. 746-751, 2010.
- [60] R. J. Hunter and L. R. White, *Foundations of colloidal science.:* Clarendon Press, 1987.
- [61] K. Mladenovska et al., "5-ASA loaded chitosan-Ca-alginate microparticles: Preparation and physicochemical characterization," vol. 345, pp. 59-69, 2007.
- [62] J. N. Israelachvili, *Intermolecular and surface forces*, Revised third ed.: Academic press, 2011.
- [63] J. -O. You et al., "Preparation of regular sized Ca-alginate microspheres using membrane emulsification method," *Journal of Microencapsulation*, vol. 18, pp. 521-532, 2001.
- [64] Q. Zhao, J. Coult, and G. H. Pollack, "Long-range attraction in aqueous colloidal suspensions," in *Proceedings of SPIE*, 7376, 2010, pp. 73761C-1-73761C-13.